Electronic Supplementary Material (ESI).
This journal is © The Royal Society of Chemistry 2021

Electronic Supplementary Information

Achieving Highly Efficient Aggregation-Induced Emission, Reversible and Irreversible Photochromism by Heavy Halogen-Regulated Photophysics and D-A Molecular Pattern-Controlled Photochemistry of Through-Space Conjugated Lumingens

Zuping Xiong, Xiaoxiao Zhang, Longxiang Liu, Qiaozhi Zhu, Zhenni Wang, Hui Feng and Zhaosheng Qian*

Key Laboratory of the Ministry of Education for Advanced Catalysis Materials, College of Chemistry and Life Sciences, Zhejiang Normal University, Jinhua 321004, People's Republic of China

Table of Contents

3.6 Figure S5. The UV-visible absorption spectra of NTPAN, NTPAN-F, NTPAN-Cl, NTPAN-Br and NTPAN-I in DCM at concentration 1.0×10^{-5} M.

3.7 Figure S6. Time-resolved fluorescence decay curves of NTPAN (a), NTPAN-F (b), NTPAN-Cl (c), NTPAN-Br (d) and NTPAN-I (e) in solid state.

3.8 Figure S7. Aggregation-induced emission behaviors of NTPAN (a), NTPAN-F (b), NTPAN-Cl (c), NTPAN-Br (d) and NTPAN-I (e) in THF/water mixtures with varying water fractions (fw).

3.9 Figure S8. Low-temperature time-resolved decay curves of TPAN-F, TPAN-Cl, TPAN-Br and TPAN-I in THF at 77 K.

3.10 Figure S9. Low-temperature time-resolved decay curves of NTPAN-F, NTPAN-Cl, NTPAN-Br and NTPAN-I in THF at 77 K.

3.11 Figure S10. (a) HOMOs and LUMOs of the TPAN derivatives. (b) HOMOs and LUMOs of the NTPAN derivatives.

3.12 Figure S11. Hirshfeld surface of NTPAN-F (a), NTPAN-Cl (b), NTPAN-Br (c) and NTPAN-I (d) mapped with parameter d_{norm} along with 2-D fingerprint plots with a specific interaction. Pie-charts: Relative contributions of various intermolecular interactions to the Hirshfeld surface area.

3.13 Figure S12. Time-resolved fluorescence decay curves of TPAN (a), TPAN-F (b), TPAN-Cl (c), TPAN-Br (d) and TPAN-I (e) in adamantane (AdH).

3.14 Figure S13. Time-resolved fluorescence decay curves of NTPAN (a), NTPAN-F (b), NTPAN-Cl (c),NTPAN-Br (d) and NTPAN-I (e) in adamantane (AdH).

3.15 Figure S14. (a) Changes in structural conformations of Type-G crystal and Type-Y crystal of NTPAN. (b) PL spectra of Type-G crystal and Type-Y crystal of NTPAN.

3.16 Figure S15. (a-e) Time-dependent UV-vis absorption spectra of NTPAN (a), NTPAN-F (b), NTPAN-Cl (c), NTPAN-Br (d), NTPAN-I (e) in DCM (2.0 mM) under continuous UV irradiation at 365 nm. **(f-g)** Time-dependent PL spectra of NTPAN (a), NTPAN-F (b), NTPAN-Cl (c), NTPAN-Br (d), NTPAN-I (e) in DCM (2.0 mM) under continuous UV irradiation at 365 nm. **(k)** Change in PL intensity of NTPAN compounds in DCM (2 mM) after 365 nm UV irradiation. **(l)** Change in PL spectra of NTPAN-F in DCM (2 mM) at various conditions: the original solution (before 365 nm UV), the photochromic solution (after 365 nm UV irradiation) and the photochromic solution (placed natural standing for 10 min) respectively.

4. Supplementary Tables

4.1 Table S1. Crystallographic data of TPAN, TPAN-F, TPAN-Cl, TPAN-Br, TPAN-I.

4.2 Table S2. Crystallographic data of NTPAN, NTPAN-F, NTPAN-Cl, NTPAN-Br and NTPAN-I.

4.3 Table S3. Photophysical properties of TPAN, TPAN-F, TPAN-Cl, TPAN-Br, TPAN-I, NTPAN, NTPAN-F, NTPAN-Cl, NTPAN-Br and NTPAN-I in different states.

4.4 Table S4. Contribution ratioes of different atoms to HOMOs and LUMOs of TPAN, TPAN-F, TPAN-Cl, TPAN-Br and TPAN-I.

4.5 Table S5. Contribution ratioes of different atoms to HOMOs and LUMOs of NTPAN, NTPAN-F, NTPAN-Cl, NTPAN-Br and NTPAN-I.

4.6 Table S6. Excitation energies of first 10 states for TPAN, TPAN-F, TPAN-Cl, TPAN-Br and TPAN-I calculated with TDDFT.

4.7 Table S7. Excitation energies of first 10 states for NTPAN, NTPAN-F, NTPAN-Cl, NTPAN-Br

5. Spectra of Compounds

5.26 High-resolution mass spectrum of 3,3-bis(4-(dimethylamino)phenyl)-2-phenylacrylonitrile (NTPAN)

5.27 High-resolution mass spectrum of 3,3-bis(4-(dimethylamino)phenyl)-2-(4-fluorophenyl) acrylonitrile (NTPAN-F)

5.28 High-resolution mass spectrum of 2-(4-chlorophenyl)-3,3-bis(4-(dimethylamino)-phenyl) acrylonitrile (NTPAN-Cl)

5.29 High-resolution mass spectrum of 2-(4-bromophenyl)-3,3-bis(4-(dimethylamino)phenyl) acrylonitrile (NTPAN-Br)

5.30 High-resolution mass spectrum of 3,3-bis(4-(dimethylamino)phenyl)-2-(4-iodophenyl) acrylonitrile (NTPAN-I)

6. References

1. Experimental Section

Synthesis of 2,3,3-triphenylacrylonitrile (TPAN). 2,3,3-Triphenylacrylonitrile was synthesized and purified according to the previous procedure in the literature.[1] Molecular formula: $C_{21}H_{15}N$. ^{1}H NMR (600 MHz, $CDCl_3$) δ 7.50-7.36 (m, 5H), 7.30-7.26 (m, 2H), 7.25-7.15 (m, 6H), 7.01 (d, J = 7.7 Hz, 2H). ^{13}C NMR (150 MHz, $CDCl_3$) δ(ppm) 157.8, 140.4, 139.1, 134.8, 130.8, 129.9, 129.9, 129.7, 129.0, 128.5, 128.4, 128.3, 128.2, 120.1, 111.6. HRMS (ESI) m/z: $[M]^+$ 281.11983, (calcd. for $C_{21}H_{15}N$, 281.12045). CCDC No. 2054237.

Synthesis of 2-(4-fluorophenyl)-3,3-diphenylacrylonitrile (TPAN-F). Benzophenone (4.00 g, 22 mmol), NaH (60%, 1 g, 25 mmol), and anhydrous dioxane (50 mL) were placed in a three-necked round-bottom flask (250 mL) equipped with a reflux condenser under nitrogen. The mixture was refluxed for 10 min, and then 2-(4-fluorophenyl)acetonitrile (2.7 g, 20 mmol) in anhydrous dioxane (60 mL) was added dropwise by injector over 60 min while maintaining reflux. Evolved H_2 was observed at the oil bubbler, and the reaction lasted for 20 h. Upon cooling to room temperature, 100 mL of water was added to the mixture, and then 250 mL of CH_2Cl_2 was then added for extraction. The organic layer was collected and washed with brine 3 times. The organic phase was dried over anhydrous $MgSO_4$ and concentrated under vacuum. The crude product was purified by column chromatography to give a colourless solid (Yield 60%). Molecular formula: $C_{21}H_{14}NF$. ^{1}H NMR (400 MHz, $CDCl_3$) δ (ppm) 7.48-7.38 (m, 5H), 7.29 -7.17 (m, 5H), 7.03-6.96 (m, 2H), 6.91 (t, J = 8.7 Hz, 2H). δ(ppm) ^{13}C NMR (100 MHz, $CDCl_3$) δ(ppm) 163.6, 161.1, 157.9, 140.2, 138.9, 131.6, 131.6, 130.9, 130.8, 130.7, 130.0, 129.9, 129.1, 128.5, 128.4, 120.0, 115.7, 115.5, 110.5. HRMS (ESI) m/z: $[M]^+$ 299.10981, (calcd. for $C_{21}H_{14}FN$, 299.11103). CCDC No. 2054250.

Synthesis of 2-(4-chlorophenyl)-3,3-diphenylacrylonitrile (TPAN-Cl). Benzophenone (4.00 g, 22 mmol), NaH (60%, 1 g, 25 mmol), and anhydrous toluene (50 mL) were added in a three-necked round-bottom flask (250 mL) equipped with a reflux condenser under nitrogen. The mixture was refluxed for 10 min, and then 2-(4-

chlorophenyl)-3,3-diphenylacrylonitrile (3.02 g, 20 mmol) in toluene (60 mL) was added dropwise over 1 h under reflux. The reaction lasted for 20 h. After cooling to room temperature, 100 mL of water was added to the mixture. The organic layer was collected and washed with brine 3 times. The organic phase was dried over anhydrous $MgSO_4$ and concentrated under vacuum. Finally, the crude product was purified by column chromatography to give a colourless solid (Yield 79%). It was recrystallized with methylene chloride and petroleum ether to get colorless crystals. Molecular formula: $C_{21}H_{14}NCl$. ^1H NMR (600 MHz, $CDCl_3$) δ (ppm) 7.47-7.39 (m, 5H), 7.28-7.25 (m, 1H), 7.24-7.14 (m, 6H), 7.00 (d, J = 7.4 Hz, 2H). ^{13}C NMR (150 MHz, $CDCl_3$) δ(ppm) 158.4, 140.1, 138.8, 134.3, 133.3, 131.0, 130.7, 130.1, 129.9, 129.2, 128.8, 128.5, 128.4, 119.8, 110.4. HRMS (ESI) m/z: $[M]^+$ 315.08036, (calcd. for $C_{21}H_{14}ClN$, 315.08148). CCDC No. 2054251.

Synthesis of 2-(4-bromophenyl)-3,3-diphenylacrylonitrile (TPAN-Br). The compound was synthesized by the same procedure described for TPAN-Cl using 2-(4-bromophenyl)acetonitrile and benzophenone. The crude product was purified by column chromatography to give a colourless solid (Yield 83%). The colorless crystals can be obtained by recrystallization with methylene chloride and petroleum ether. Molecular formula: $C_{21}H_{14}NBr$. ^1H NMR (600 MHz, $CDCl_3$) δ (ppm) 7.48-7.38 (m, 5H), 7.34 (d, J = 8.5 Hz, 2H), 7.28 (t, J = 7.4 Hz, 1H), 7.22 (t, J = 7.6 Hz, 2H), 7.12 (d, J = 8.5 Hz, 2H), 7.00 (d, J = 7.4 Hz, 2H). ^{13}C NMR (150 MHz, $CDCl_3$) δ(ppm) 158.4, 140.1, 138.7, 133.8, 131.7, 131.3, 130.7, 130.1, 129.9, 129.3, 128.5, 128.4, 122.6, 119.7, 110.4. HRMS (ESI) m/z: $[M]^+$ 359.02977, (calcd. for $C_{21}H_{14}NBr$, 359.03096). CCDC No. 2054252.

Synthesis of 2-(4-iodophenyl)-3,3-diphenylacrylonitrile (TPAN-I). The compound was synthesized by the same procedure described for TPAN-Cl using 2-(4-iodophenyl))acetonitrile and benzophenone. The crude product was purified by column chromatography to give a colourless solid (Yield 82%). The colorless crystals can be obtained by recrystallization with methylene chloride and petroleum ether. Molecular

formula: $C_{21}H_{14}IN$. ^{1}H NMR (600 MHz, $CDCl_3$) δ (ppm) 7.54 (d, J = 8.4 Hz, 2H), 7.48-7.37 (m, 5H), 7.28 (t, J = 7.4 Hz, 1H), 7.21 (t, J = 7.6 Hz, 2H), 7.00-6.96 (m, 4H). ^{13}C NMR (150 MHz, $CDCl_3$) δ(ppm) 158.4, 140.2, 138.7, 137.7, 134.4, 131.4, 130.7, 130.1, 129.9, 129.3, 128.5, 128.5, 119.7, 110.5, 94.4. HRMS (ESI) m/z: $[M]^+$ 407.01554, (calcd. for $C_{21}H_{14}IN$, 407.25447). CCDC No. 2054253.

Synthesis of 3,3-bis(4-(dimethylamino)phenyl)-2-phenylacrylonitrile (NTPAN). 4,4'-(Dimethylamino)benzophenone (5.90 g, 22 mmol), NaH (60%, 1 g, 25 mmol), and anhydrous toluene (50 mL) were placed in a three-necked round-bottom flask (250 mL) equipped with a reflux condenser under nitrogen. The mixture was refluxed for 10 min, and then 2-phenylacetonitrile(2.3 g, 20 mmol) in anhydrous toluene (60 mL) was added dropwise by injector over 60 min while maintaining reflux. Evolved H_2 was observed at the oil bubbler, and the reaction lasted for 20 h. After cooling to room temperature, 100 mL of water was added to the mixture. The organic layer was collected and washed with brine 3 times. The organic phase was dried over anhydrous $MgSO_4$ and concentrated under vacuum. Finally, the crude product was purified by column chromatography to give a yellow solid (Yield 80%). The yellow crystals can be easily obtained by recrystallization in acetone. Molecular formula: $C_{25}H_{25}N_3$. ^{1}H NMR (600 MHz, $CDCl_3$) δ (ppm) 7.39 (d, J = 8.9 Hz, 2H), 7.33 (d, J = 7.4 Hz, 2H), 7.23 (t, J = 7.6 Hz, 2H), 7.17 (t, J = 7.3 Hz, 1H), 6.92 (d, J = 8.9 Hz, 2H), 6.71 (d, J = 8.9 Hz, 2H), 6.48 (d, J = 8.9 Hz, 2H), 3.05 (s, 6H), 2.97 (s, 6H). ^{13}C NMR (150 MHz, $CDCl_3$) δ(ppm) 151.4, 150.5, 136.8, 133.0, 132.0, 129.7, 128.3, 127.0, 111.1, 110.9, 40.2, 40.1. HRMS (ESI) m/z: $[M]^+$ 367.20336, (calcd. for $C_{25}H_{25}N_3$, 367.20485).

Synthesis of 3,3-bis(4-(dimethylamino)phenyl)-2-(4-fluorophenyl)acrylonitrile (NTPAN-F). 4,4'-(Dimethylamino)benzophenone (5.90 g, 22 mmol), NaH (60%, 1 g, 25 mmol), and anhydrous dioxane (50 mL) were placed in a three-necked round-bottom flask (250 mL) equipped with a reflux condenser under nitrogen. The mixture was refluxed for 10 min and then 2-(4-fluorophenyl)acetonitrile(2.7 g, 20 mmol) in anhydrous

dioxane (60 mL) was added dropwise by injector over 60 min while maintaining reflux. Evolved H_2 was observed at the oil bubbler, and the reaction lasted for 20 h. After cooling to room temperature, 100 mL of water was added to the mixture and then 250 mL of CH_2Cl_2 was added. The organic layer was collected and washed with brine 3 times. The organic phase was dried over anhydrous $MgSO_4$ and concentrated under vacuum. Then, the crude product was purified by column chromatography to give a yellow solid (Yield 59%). Molecular formula: $C_{25}H_{24}N_3F$. ^{1}H NMR (400 MHz, $CDCl_3$) δ (ppm) 7.36 (d, J = 8.9 Hz, 2H), 7.29-7.26 (m, 1H), 7.25 (d, J = 2.3 Hz, 1H), 6.92-6.85 (m, 4H), 6.68 (d, J = 8.9 Hz, 2H), 6.46 (d, J = 8.9 Hz, 2H), 3.02 (s, 6H), 2.95 (s, 6H). ^{13}C NMR (100 MHz, $CDCl_3$) δ(ppm) 162.8, 158.8, 151.5, 150.6, 133.0, 132.8, 132.0, 131.4, 131.3, 128.0, 126.3, 122.3, 115.4, 115.2, 111.1, 111.0, 103.2, 40.2, 40.1. HRMS (ESI) m/z: $[M]^+$ 385.19379, (calcd. for $C_{25}H_{24}FN_3$, 385.19543). CCDC No. 2054256.

Synthesis of 2-(4-chlorophenyl)-3,3-bis(4-(dimethylamino)phenyl)acrylonitrile (NTPAN-Cl). Under a nitrogen atmosphere, in a three-necked round-bottom flask (250 mL) equipped with a reflux condenser was placed a mixture of 4,4'-(dimethylamino)benzophenone (5.90 g, 22 mmol), NaH (60%, 1 g, 25 mmol) and anhydrous toluene (50 mL). The mixture was refluxed for 10 min. Then, 2-(4-chlorophenyl)-3,3-diphenylacrylonitrile (3.02 g, 20 mmol) in anhydrous toluene (60 mL) was added dropwise by injector over 60 min while maintaining reflux. The reaction lasted for 20 h. After cooling to room temperature, 150 mL of water was added to the mixture and stirred for 15 minutes to precipitate large quantities of solids, which are filtered directly. Then, the crude product was purified 3 times by recrystallization in acetone to give a yellow crystal (Yield 78%). Molecular formula: $C_{25}H_{24}N_3Cl$. ^{1}H NMR (600 MHz, $CDCl_3$) δ (ppm) 7.36 (d, J = 8.8 Hz, 2H), 7.22 (d, J = 8.0 Hz, 2H), 7.17 (d, J = 8.1 Hz, 2H), 6.88 (d, J = 8.8 Hz, 2H), 6.68 (d, J = 8.8 Hz, 2H), 6.47 (d, J = 8.8 Hz, 2H), 3.03 (s, 6H), 2.96 (s, 6H). ^{13}C NMR (150 MHz, $CDCl_3$) δ(ppm) 159.3, 151.6, 150.7, 135.4, 133.0, 132.6, 132.1, 130.9, 128.5, 127.9, 126.2, 122.1, 111.1, 111.0, 102.9, 40.1, 40.0. HRMS

(ESI) m/z: $[M]^+$ 401.16430, (calcd. for $C_{25}H_{24}N_3Cl$, 401.16588). CCDC No. 2054257.

Synthesis of 2-(4-bromophenyl)-3,3-bis(4-(dimethylamino)phenyl)acrylonitrile (NTPAN-Br). The synthetic procedure for NTPAN-Br is similar to that of NTPAN-Cl described above using 2-(4-bromophenyl)-3,3-diphenylacrylonitrile instead of 2-(4-chlorophenyl)-3,3-diphenylacrylonitrile. A green crystal was obtained in 70% yield via solvent evaporation. Molecular formula: $C_{25}H_{24}N_3Br$. ^1H NMR (600 MHz, $CDCl_3$) δ (ppm) 7.51 (d, J = 8.2 Hz, 2H), 7.35 (d, J = 8.6 Hz, 2H), 7.03 (d, J = 8.2 Hz, 2H), 6.88 (d, J = 8.6 Hz, 2H), 6.68 (d, J = 8.7 Hz, 2H), 6.47 (d, J = 8.6 Hz, 2H), 3.02 (s, 6H), 2.97 (s, 6H). ^{13}C NMR (150 MHz, $CDCl_3$) δ(ppm) 159.4, 151.6, 150.7, 137.3, 136.5, 133.0, 132.1, 131.4, 127.9, 126.1, 122.0, 111.1, 111.0, 102.9, 92.4, 40.1, 40.1. HRMS (ESI) m/z: $[M]^+$ 445.11376, (calcd. for $C_{25}H_{24}N_3Br$, 445.11536). CCDC No. 2054254.

Synthesis of 3,3-bis(4-(dimethylamino)phenyl)-2-(4-iodophenyl)acrylonitrile (NTPAN-I). The synthetic procedure for NTPAN-I is similar to that of NTPAN-Cl described above using 2-(4-iodophenyl)-3,3-diphenylacrylonitrile instead of 2-(4-chlorophenyl)-3,3-diphenylacrylonitrile. A green crystal was obtained in 68% yield via solvent evaporation. Molecular formula: $C_{25}H_{24}N_3I$. ^1H NMR (600 MHz, $CDCl_3$) δ (ppm) 7.35 (d, J = 8.5 Hz, 2H), 7.32 (d, J = 8.5 Hz, 2H), 7.16 (d, J = 8.4 Hz, 2H), 6.88 (d, J = 8.7 Hz, 2H), 6.68 (d, J = 8.7 Hz, 2H), 6.47 (d, J = 8.7 Hz, 2H), 3.03 (s, 6H), 2.96 (s, 6H). ^{13}C NMR (150 MHz, $CDCl_3$) δ(ppm) 159.4, 151.6, 150.7, 135.9, 133.0, 132.1, 131.4, 131.2, 127.9, 126.2, 122.0, 120.8, 111.1, 111.0, 102.9, 40.1, 40.1. HRMS (ESI) m/z: $[M]^+$ 493.09944, (calcd. for $C_{25}H_{24}N_3I$, 493.10149). CCDC No. 2054255.

Characterization of UV-Visible and Fluorescence Properties of All Samples. UV−vis absorption spectra were recorded using an Agilent Cary 5000 UV-Vis-NIR spectrophotometer. Steady PL spectra of all samples were performed on an Edinburgh Instruments model FLS980 fluorescence spectrophotometer equipped with a xenon arc lamp using a front face sample holder. Time-resolved fluorescence measurements were conducted with EPL-series lasers. The absolute PL quantum yields of all samples were

determined using an integrating sphere equipped in FLS980 spectrophotometer for at least three times. For the photochromism experiments, the UV-light lamp source used in the experiment was a hand-held UV lamp with 8 w (254 nm and 365 nm); the wattage of the white light source which was from the flashlight of iphone used in the experiment was 1 W. The experimental details for reversible/irreversible photochromism on solid surface: (1) the TPAN (or NTPAN) and sucrose octaacetate were dissolved in DCM at a mass ratio of 1:100; (2) the solid materials were soaked for a few seconds and then taken out to dry naturally; (3) finally, sucroseoctaacetate and TPAN/NTPAN can form a photochromic thin film on the surface of these materials such as cotton, cellulose and paper.

2. Computational Details

All the calculations were performed with density functional theory (DFT) and time-dependent density functional theory (TDDFT) implemented in Gaussian 09 program package.[2] The ground state equilibrium geometries and the normal modes of vibration of the single-molecules of all compounds were computed using density functional theory (DFT) with the hybrid B3LYP functional at 6-311+G(d,p) level for C, N, F, Cl and H, and at LanL2DZ level for Br and I.[3] SCRF model was used to simulate the solvent effect. NBO analysis of all the compounds and their photocyclized products were performed with the same basis set to the optimization. Excitation energies and absorption maxima of all the molecules were calculated using PBE0 functional based on the optimized structures in DCM with SCRF.[4] Taken TPAN and NTPAN as examples, the independent gradient model (IGM) method was used on the basis of a single crystal structure to visualize such through-space interactions.[5] In order to observe the intermolecular forces of TPAN, NTPAN and their halogenated derivatives more clearly, theoretical investigation of intermolecular interactions in the crystal structures of these molecules are investigated via Hirsh-feld surface analysis (Isovalue: 0.5) using Crystal Explorer.[6] The vibration intensity is observed via the GuassView 6.0.

3. Supplementary Schemes and Figures

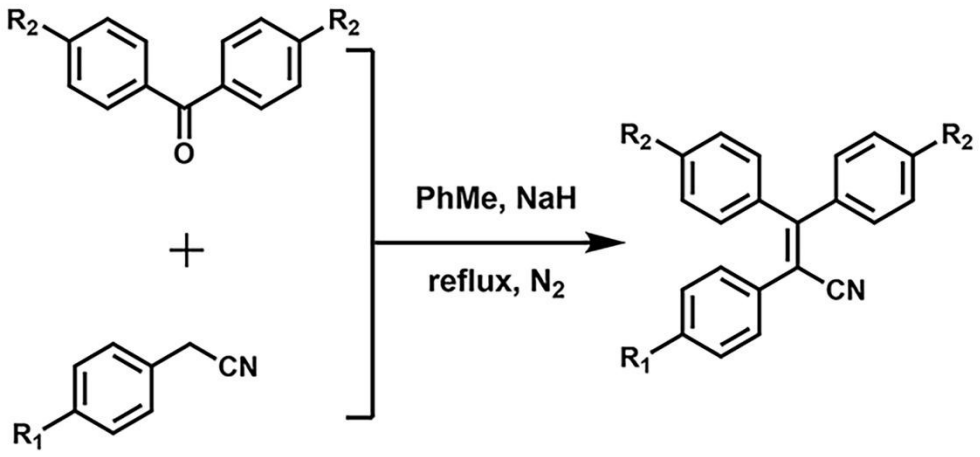

$R_1 = R_2 = H$		TPAN	$R_2 = NMe_2$	$R_1 = H$	NTPAN
$R_1 = F$	$R_2 = H$	TPAN-F	$R_2 = NMe_2$	$R_1 = F$	NTPAN-F
$R_1 = Cl$	$R_2 = H$	TPAN-Cl	$R_2 = NMe_2$	$R_1 = Cl$	NTPAN-Cl
$R_1 = Br$	$R_2 = H$	TPAN-Br	$R_2 = NMe_2$	$R_1 = Br$	NTPAN-Br
$R_1 = I$	$R_2 = H$	TPAN-I	$R_2 = NMe_2$	$R_1 = I$	NTPAN-I

Scheme S1. Synthesis routes of TPAN, TPAN-F, TPAN-Cl, TPAN-Br, TPAN-I, NTPAN, NTPAN-F, NTPAN-Cl, NTPAN-Br and NTPAN-I.

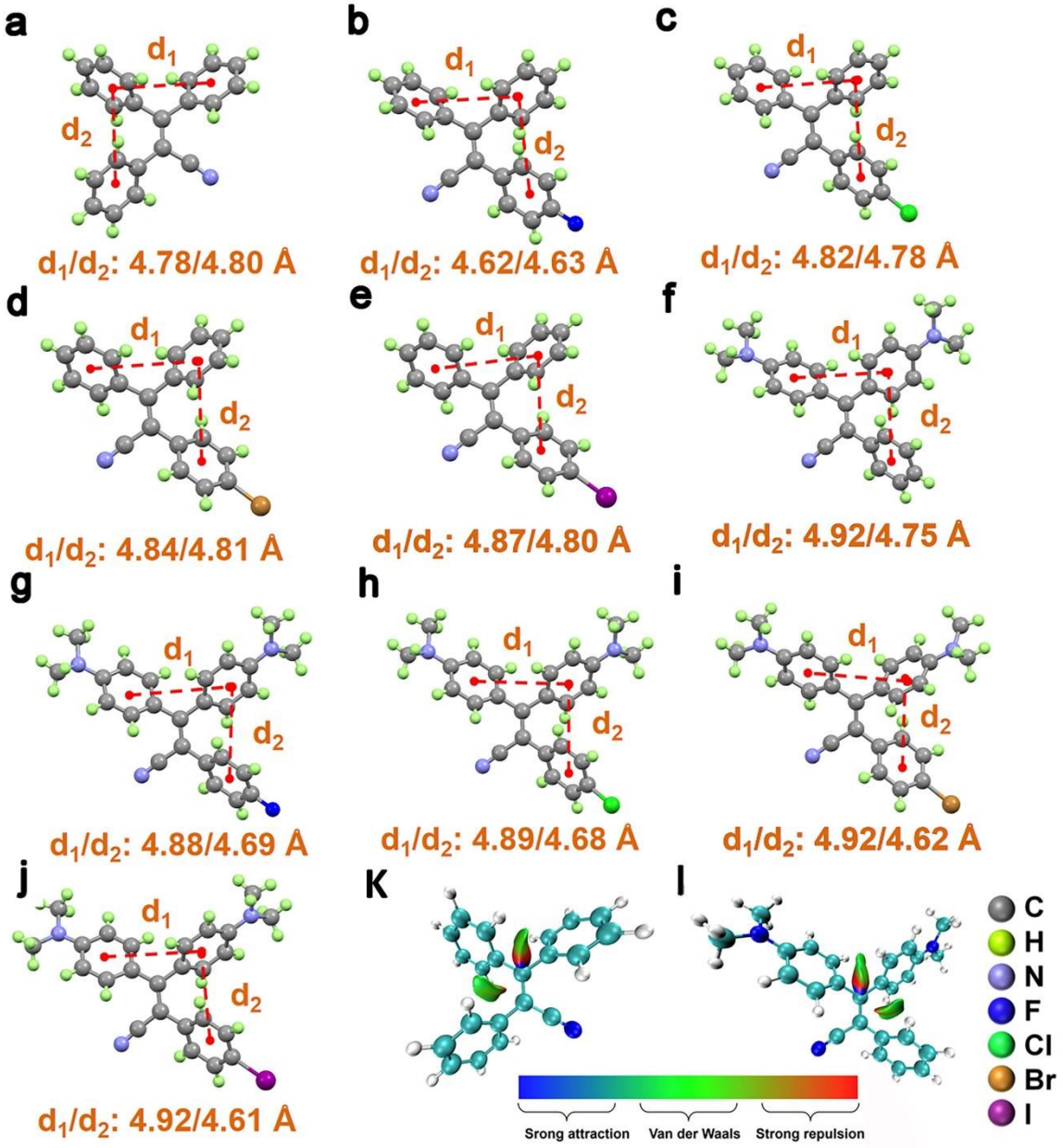

Figure S1. Absolute structures of TPAN (a), TPAN-F (b), TPAN-Cl (c), TPAN-Br (d), TPAN-I (e), NTPAN (f), NTPAN-F (g), NTPAN-Cl (h), NTPAN-Br (i) and NTPAN-I (j) with labeled distances between two intramolecular adjacent conjugated units determined by single-crystal X-ray diffraction, and the visualization of through-space conjugation of TPAN (k) and NTPAN (l) skeleton visualized by the independent gradient model (IGM) method.

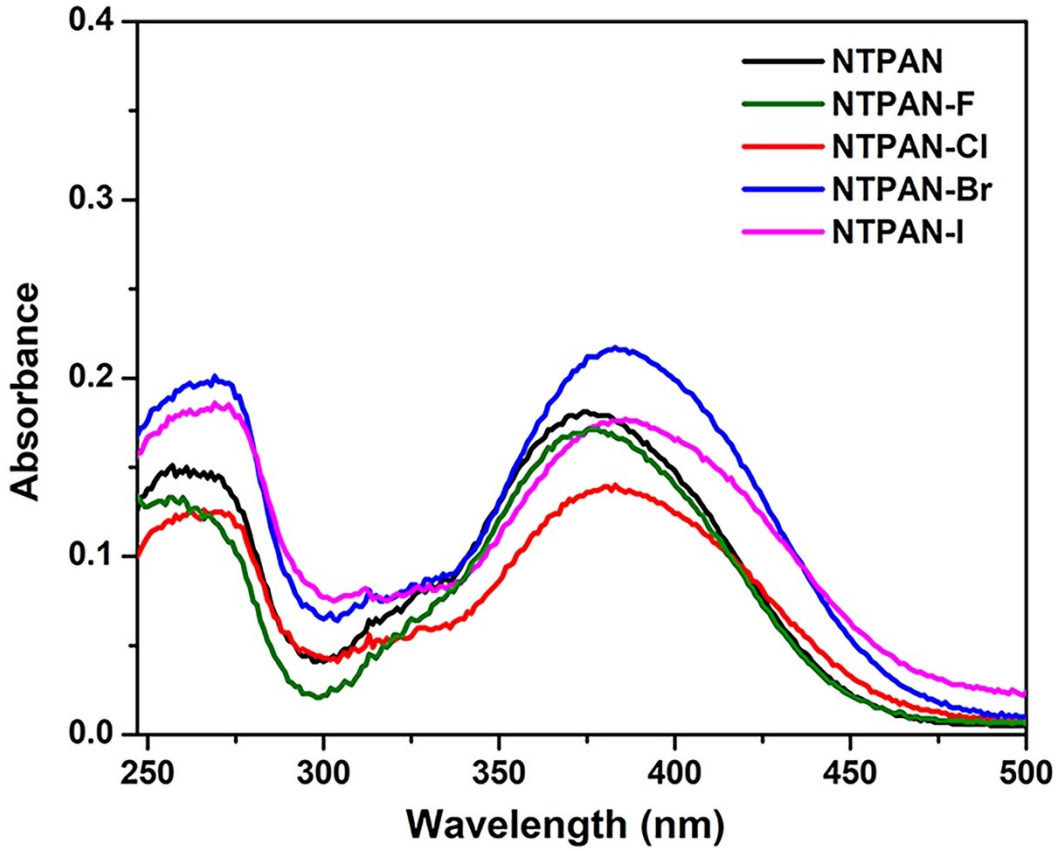

Figure S2. The UV-visible absorption spectra of TPAN, TPAN-F, TPAN-Cl, TPAN-Br and TPAN-I in DCM at concentration 1.0×10^{-5} M.

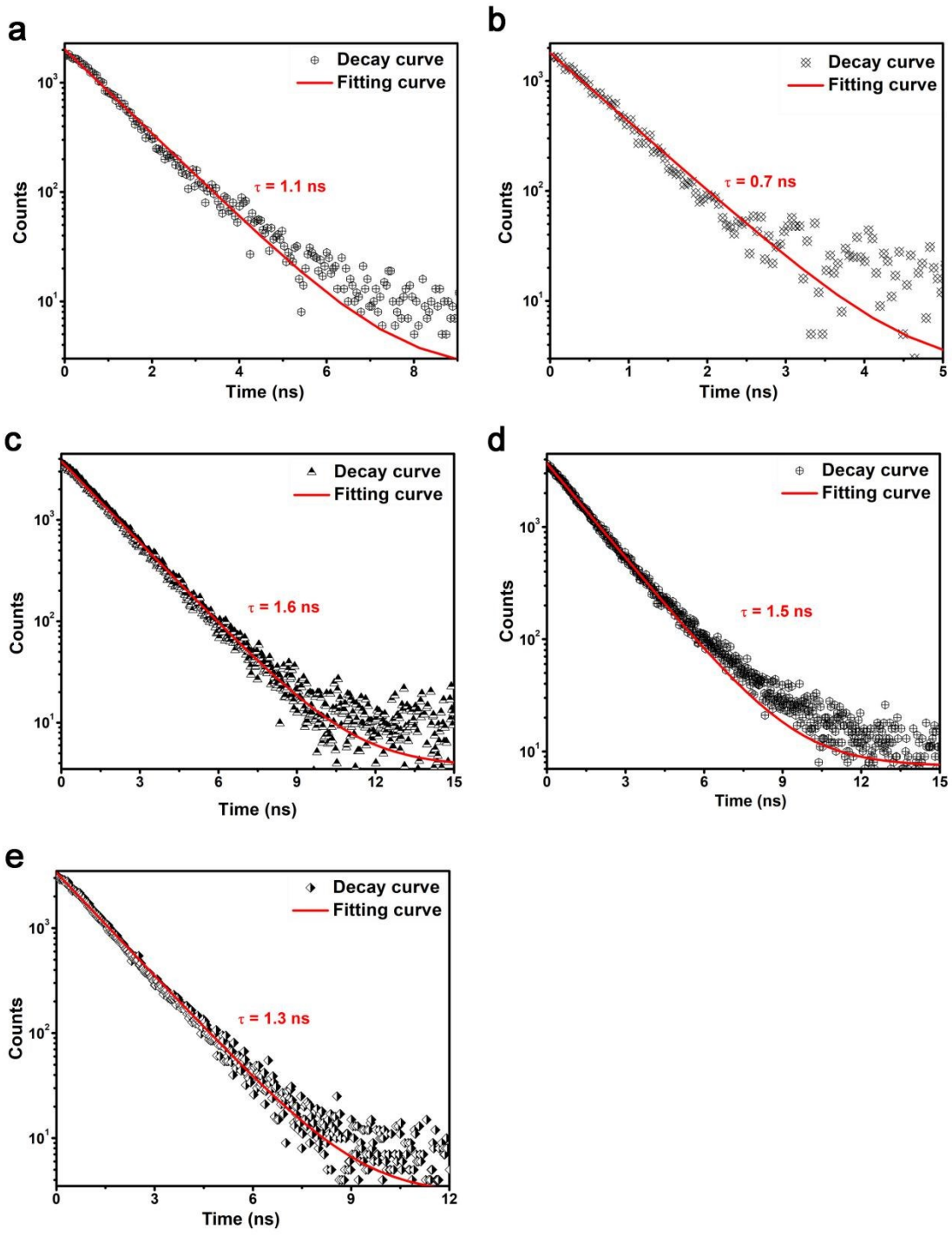

Figure S3. Time-resolved fluorescence decay curves of TPAN (a), TPAN-F (b), TPAN-Cl (c), TPAN-Br (d) and TPAN-I (e) in solid state at 298 K. (λ_{ex} = 380 nm; λ_{em} = 468, 467, 468, 474 and 475 nm for TPAN (a), TPAN-F (b), TPAN-Cl (c), TPAN-Br (d) and TPAN-I (e) respectively)

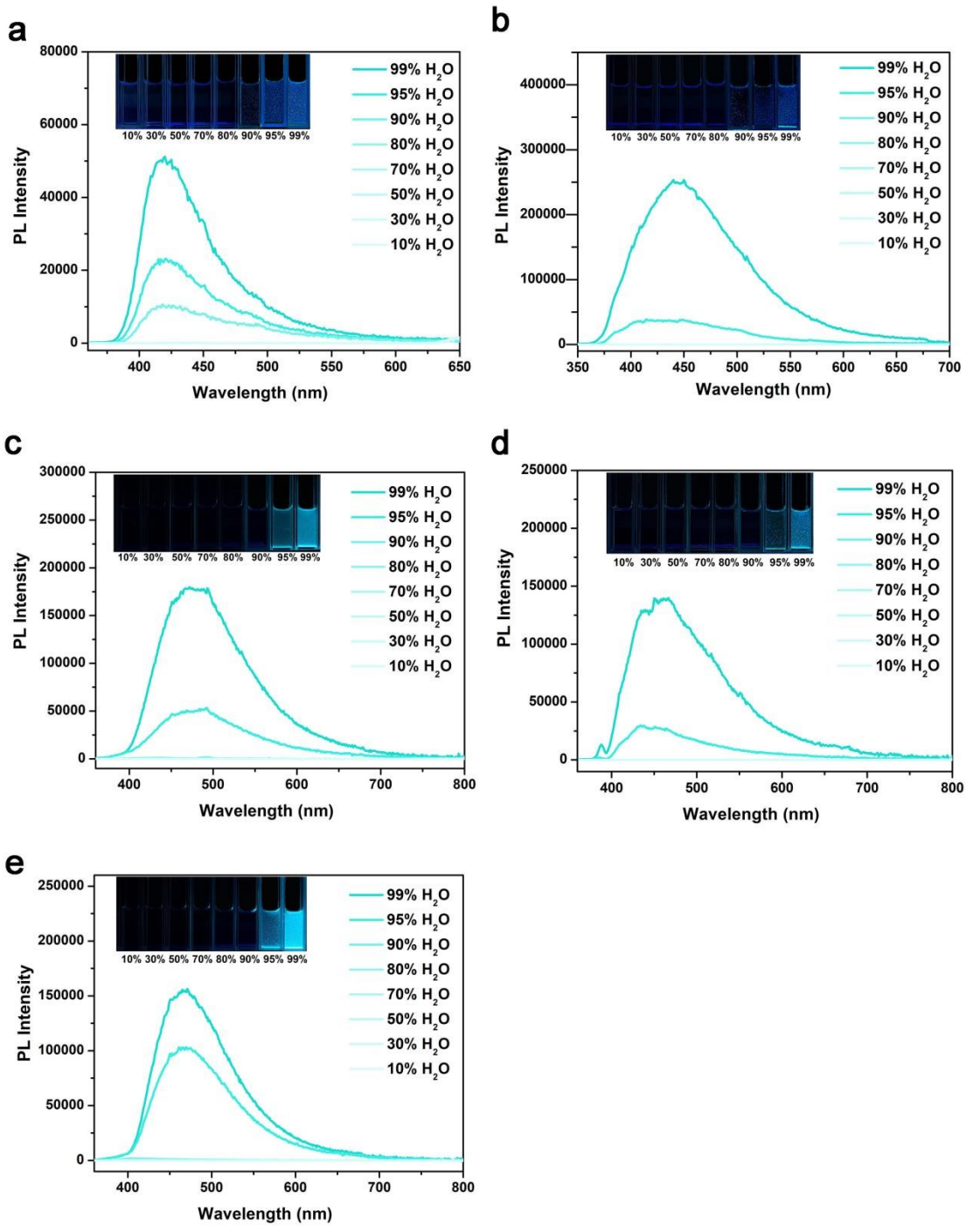

Figure S4. Aggregation-induced emission behaviors of TPAN (a), TPAN-F (b), TPAN-Cl (c), TPAN-Br (d) and TPAN-I (e) in THF/water mixtures with varying water fractions (fw).

Figure S5. The UV-visible absorption spectra of NTPAN, NTPAN-F, NTPAN-Cl, NTPAN-Br and NTPAN-I in DCM at concentration 1.0×10^{-5} M.

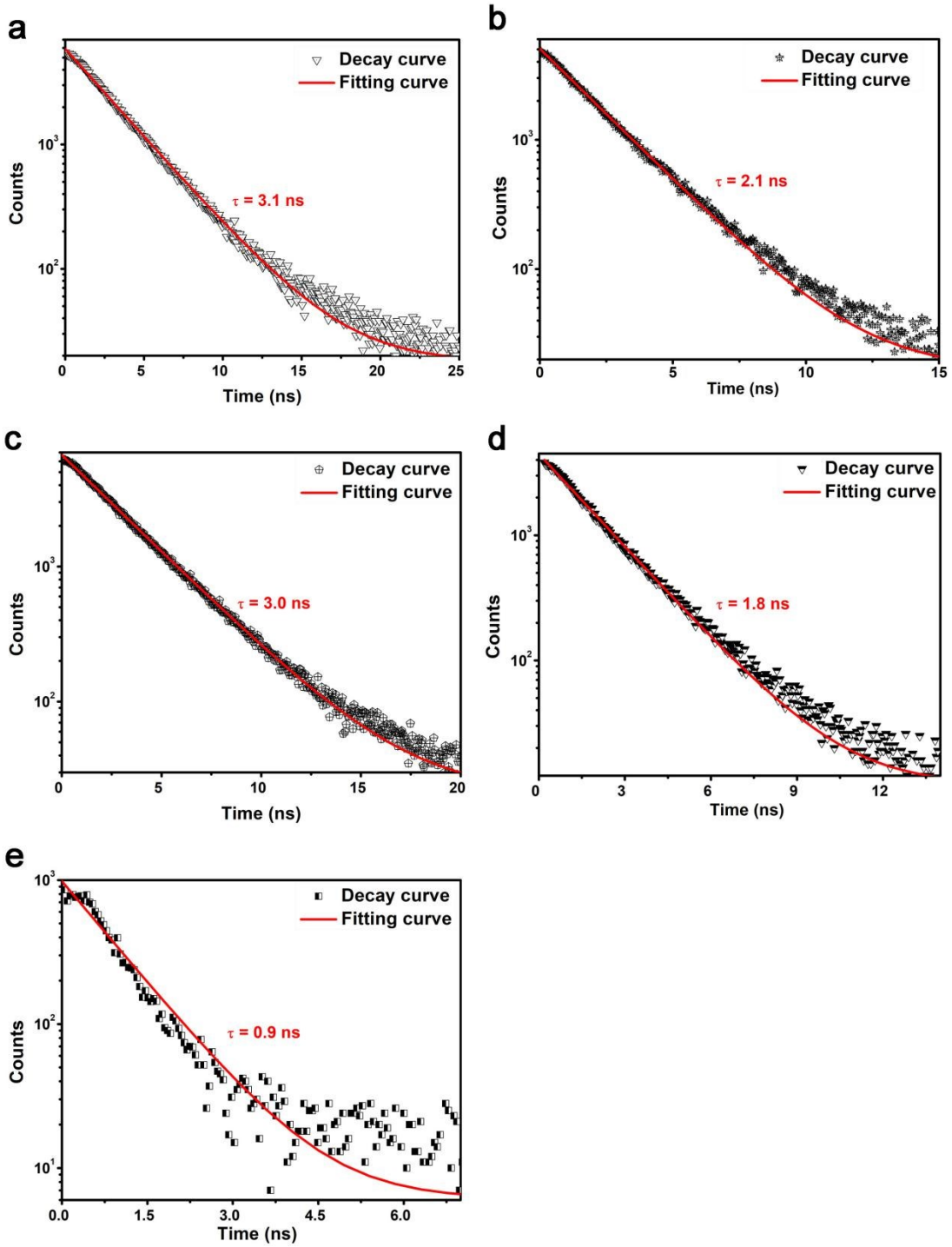

Figure S6. Time-resolved fluorescence decay curves of NTPAN (a), NTPAN-F (b), NTPAN-Cl (c), NTPAN-Br (d) and NTPAN-I (e) in solid state at 298 K. (λ_{ex} = 380 nm; λ_{em} = 590, 542, 575, 520 and 561 nm for NTPAN (a), NTPAN-F (b), NTPAN-Cl (c), NTPAN-Br (d) and NTPAN-I (e) respectively)

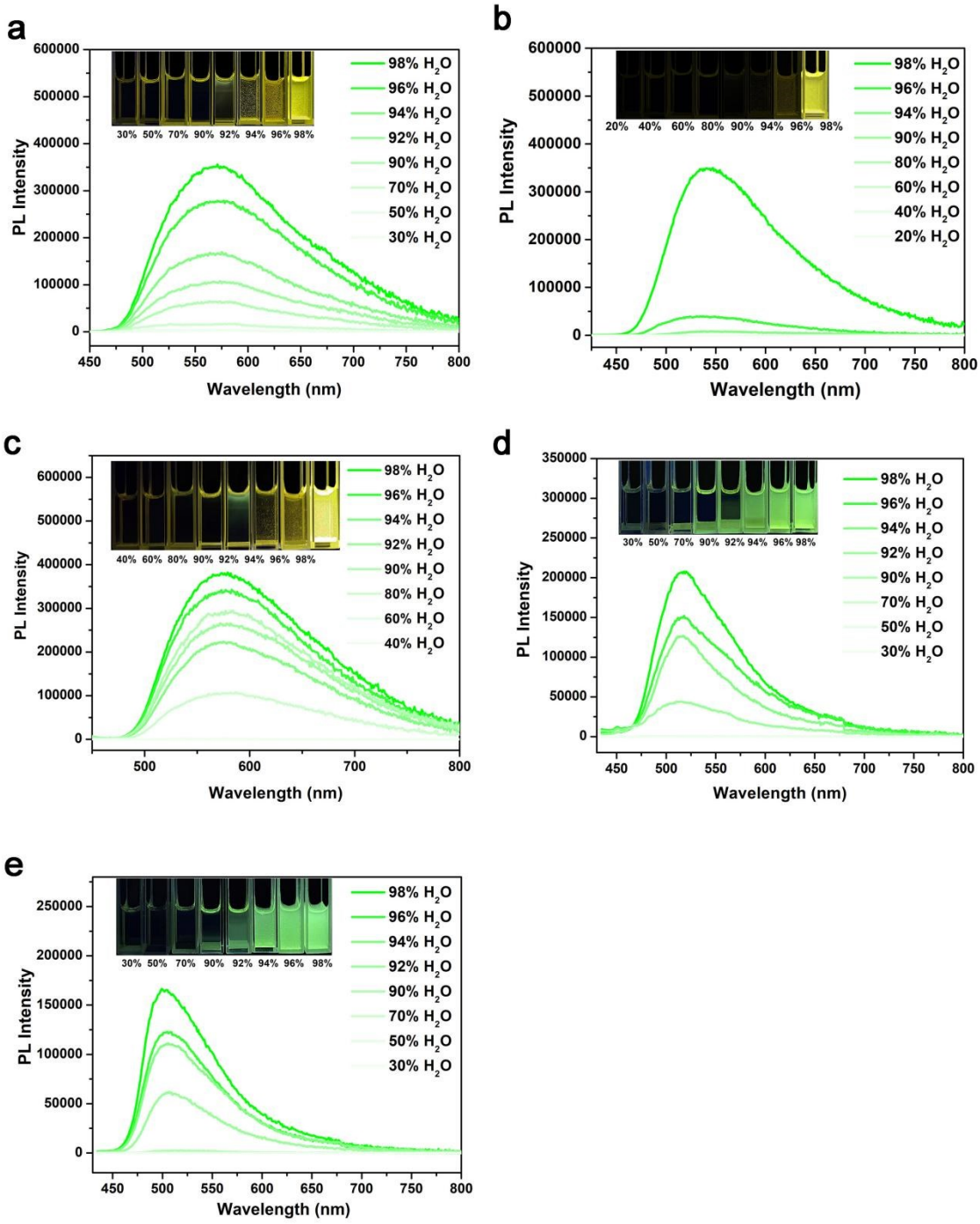

Figure S7. Aggregation-induced emission behaviors of NTPAN (a), NTPAN-F (b), NTPAN-Cl (c), NTPAN-Br (d) and NTPAN-I (e) in THF/water mixtures with varying water fractions (fw).

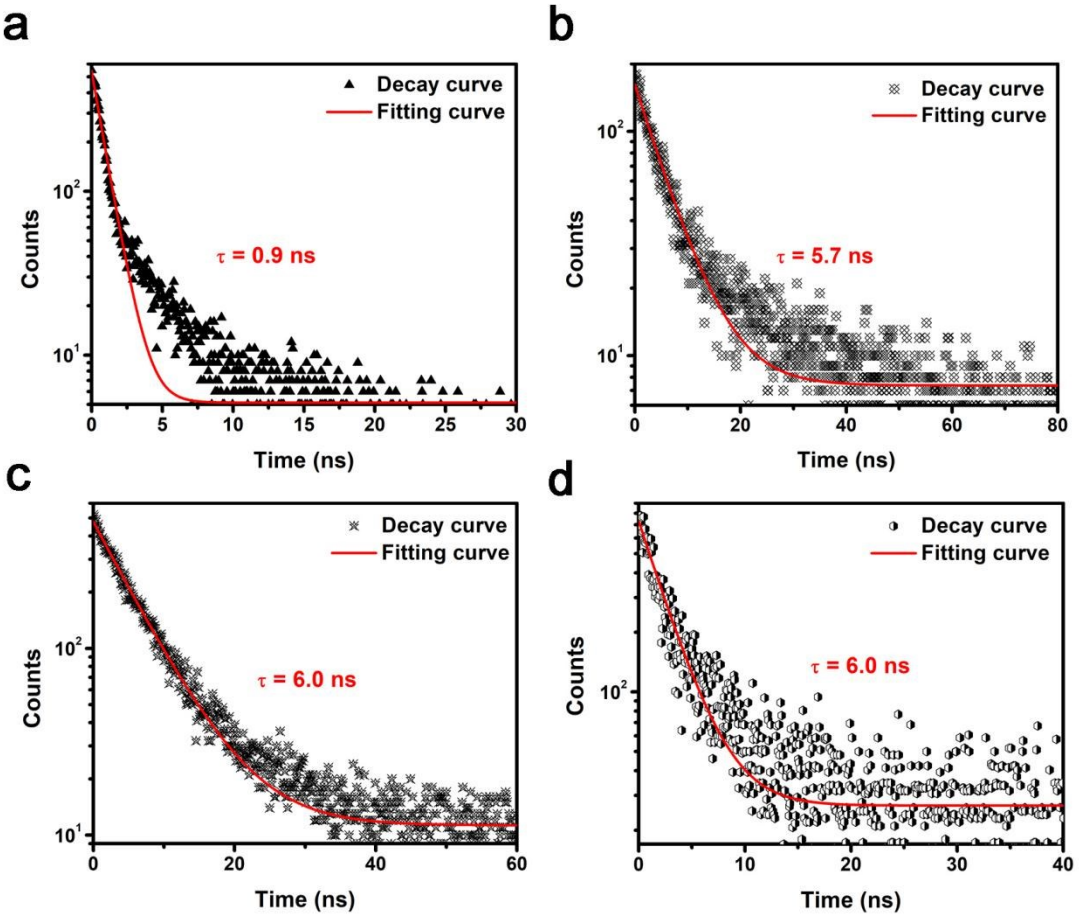

Figure S8. Low-temperature time-resolved decay curves of TPAN-F, TPAN-Cl, TPAN-Br and TPAN-I in THF at 77 K. (λ_{ex} = 380 nm; λ_{em} = 475, 450, 440 and 489 nm for TPAN (a), TPAN-F (b), TPAN-Cl (c), TPAN-Br (d) and TPAN-I (e) respectively)

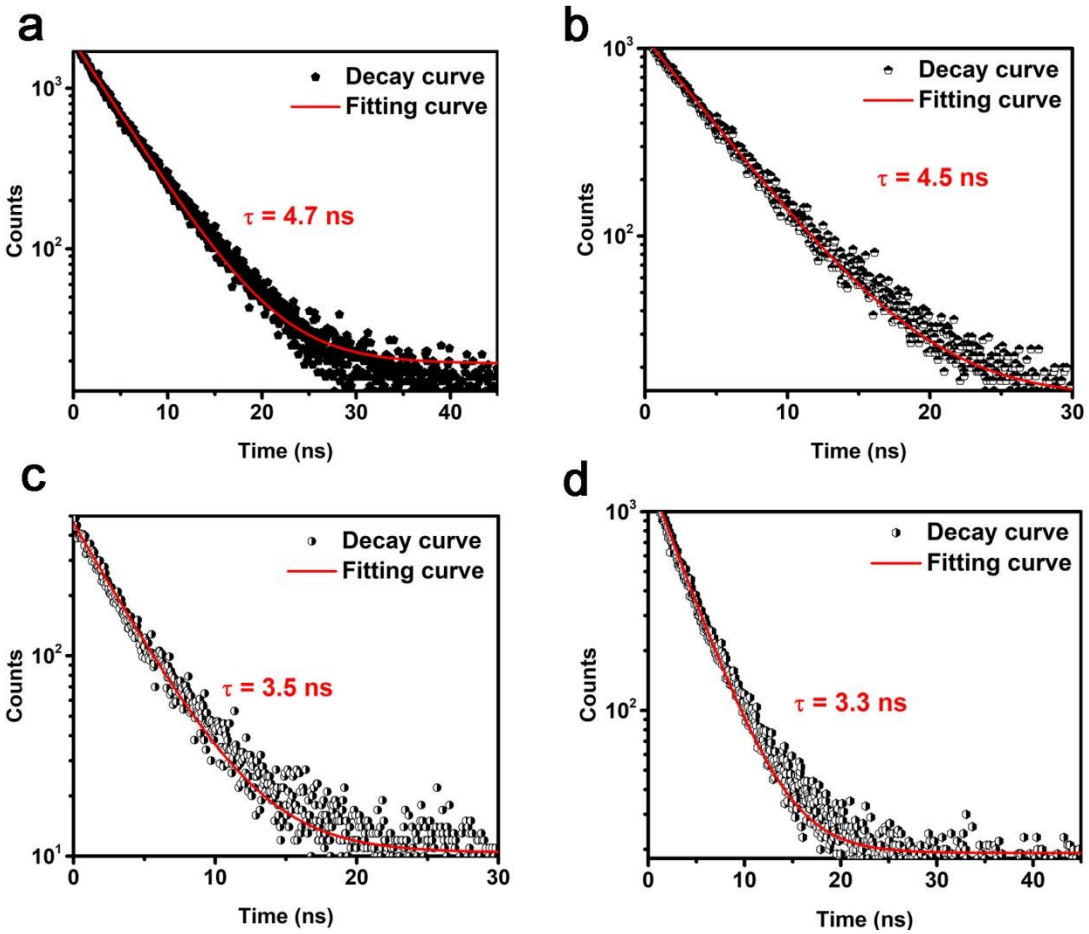

Figure S9. Low-temperature time-resolved decay curves of NTPAN-F, NTPAN-Cl, NTPAN-Br and NTPAN-I in THF at 77 K. (λ_{ex} = 380 nm; λ_{em} = 547, 556, 570 and 539 nm for NTPAN (a), NTPAN-F (b), NTPAN-Cl (c), NTPAN-Br (d) and NTPAN-I (e) respectively)

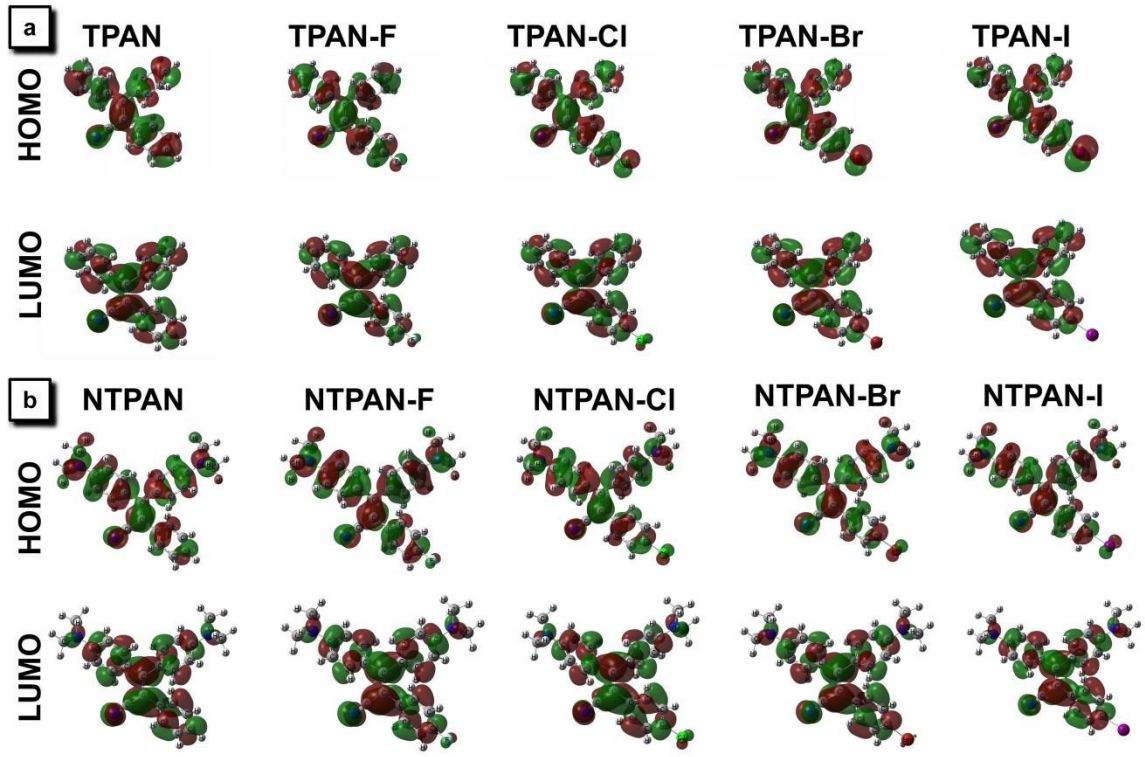

Figure S10. (a) HOMOs and LUMOs of the TPAN derivatives. (b) HOMOs and LUMOs of the NTPAN derivatives.

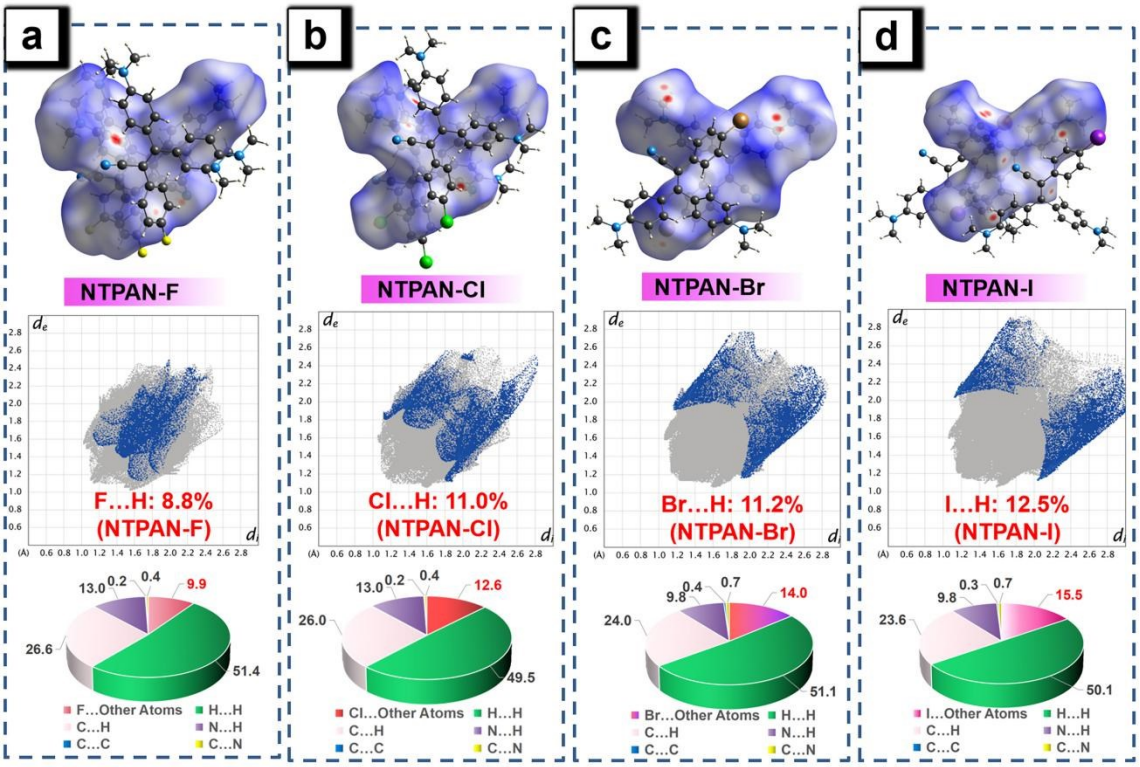

Figure S11. Hirshfeld surfaces of NTPAN-F (a), NTPAN-Cl (b), NTPAN-Br (c) and NTPAN-I (d) mapped with parameter d_{norm} along with 2-D fingerprint plots with a specific interaction. Pie-charts: Relative contributions of various intermolecular interactions to the Hirshfeld surface area.

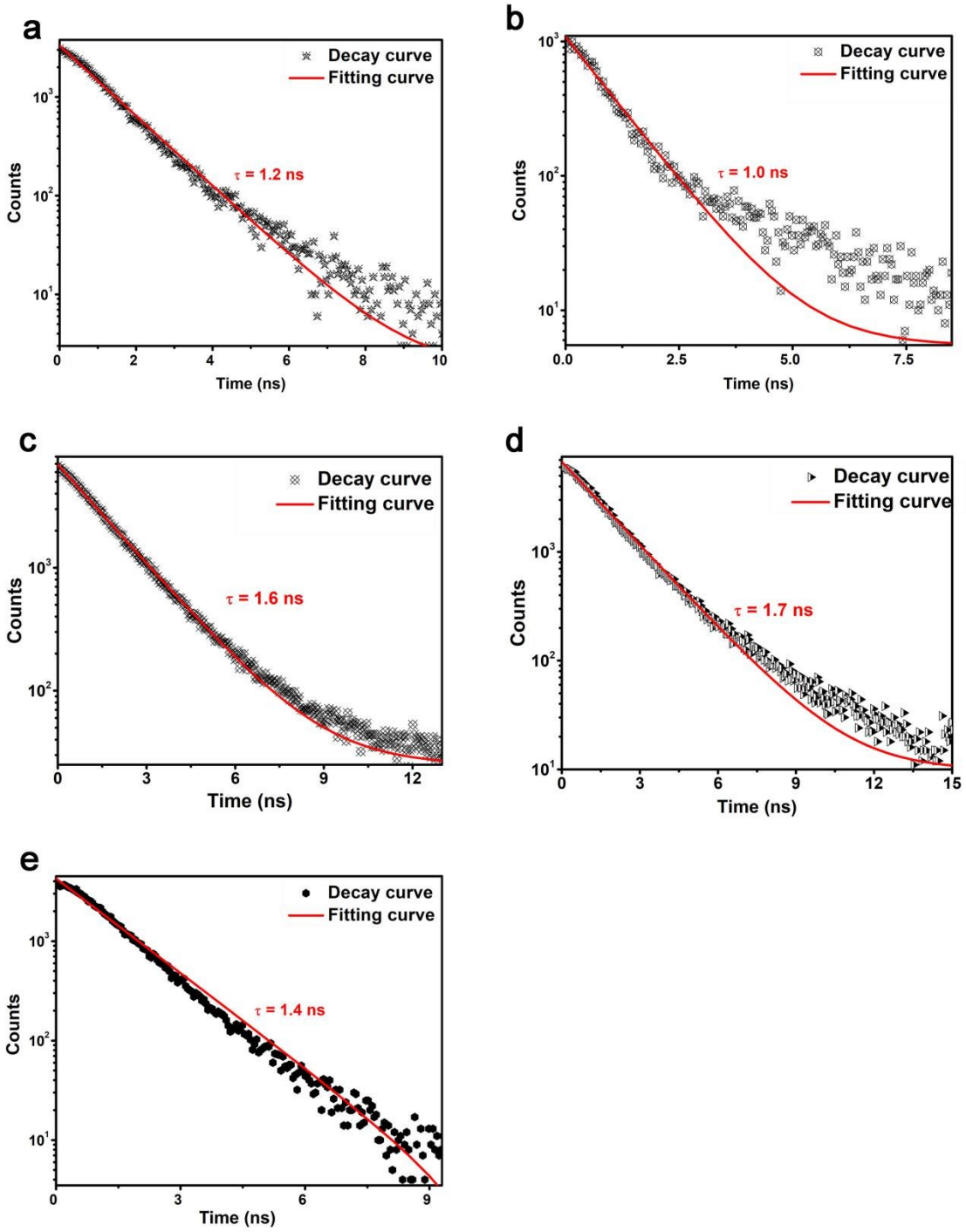

Figure S12. Time-resolved fluorescence decay curves of TPAN (a), TPAN-F (b), TPAN-Cl (c), TPAN-Br (d) and TPAN-I (e) in adamantane (AdH) at 298 K. (λ_{ex} = 380 nm; λ_{em} = 444, 467, 468, 469 and 467 nm for TPAN (a), TPAN-F (b), TPAN-Cl (c), TPAN-Br (d) and TPAN-I (e) respectively)

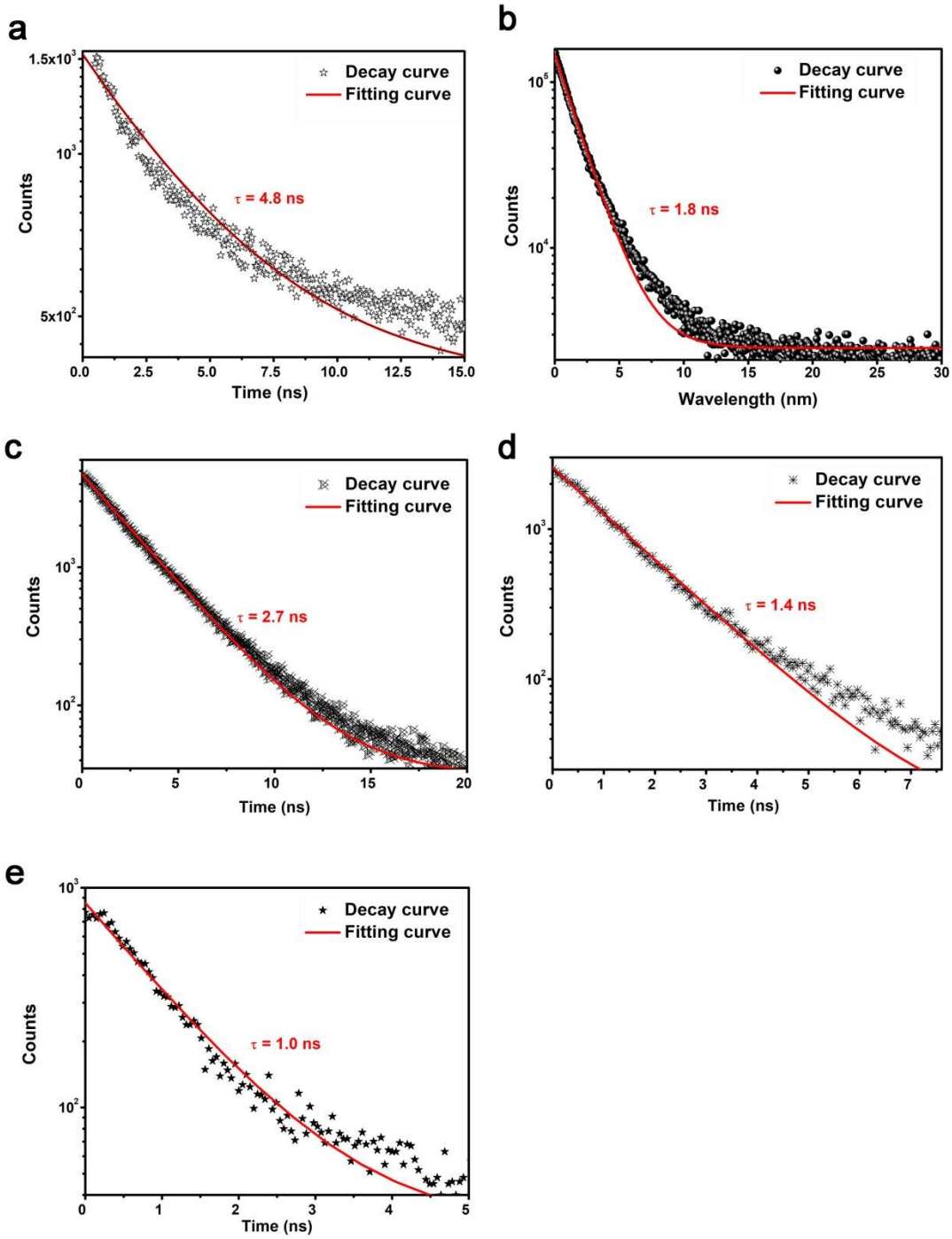

Figure S13. Time-resolved fluorescence decay curves of NTPAN (a), NTPAN-F (b), NTPAN-Cl (c),NTPAN-Br (d) and NTPAN-I (e) in adamantane (AdH) at 298 K. (λ_{ex} = 380 nm; λ_{em} = 494, 500, 558, 515 and 571 nm for NTPAN (a), NTPAN-F (b), NTPAN-Cl (c), NTPAN-Br (d) and NTPAN-I (e) respectively)

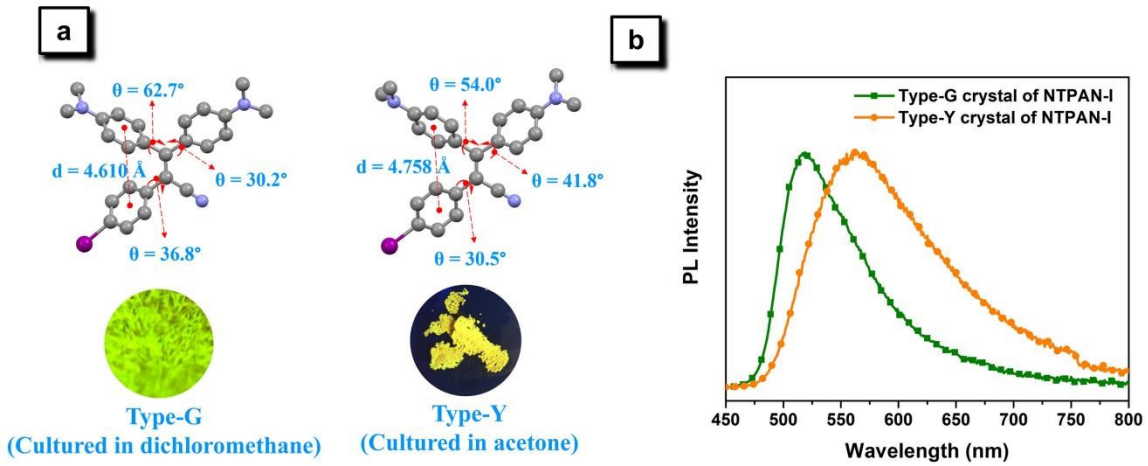

Figure S14. (a) Changes in structural conformations of Type-G crystal and Type-Y crystal of NTPAN. (b) PL spectra of Type-G crystal and Type-Y crystal of NTPAN.

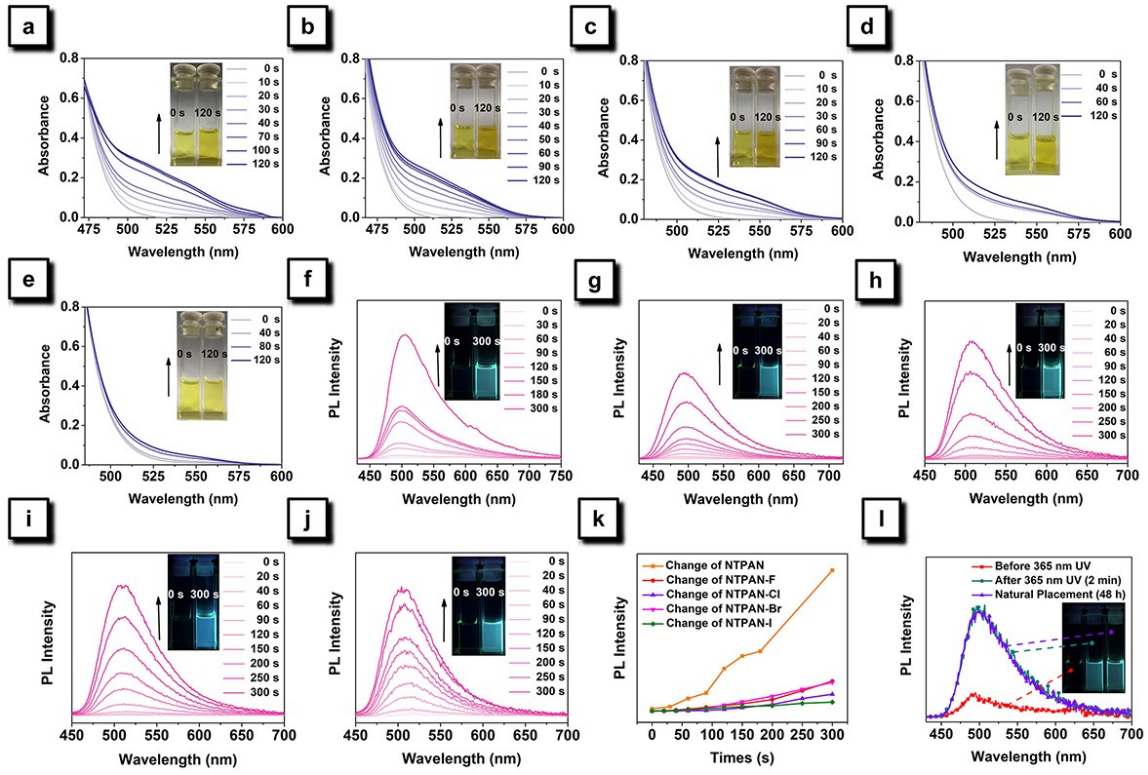

Figure S15. (a-e) Time-dependent UV-vis absorption spectra of NTPAN (a), NTPAN-F (b), NTPAN-Cl (c), NTPAN-Br (d), NTPAN-I (e) in DCM (2.0 mM) under continuous UV irradiation at 365 nm. **(f-j)** Time-dependent PL spectra of NTPAN (f), NTPAN-F (g), NTPAN-Cl (h), NTPAN-Br (i), NTPAN-I (j) in DCM (2.0 mM) under continuous UV irradiation at 365 nm. **(k)** Change in PL intensity of NTPAN compounds in DCM (2.0

mM) after 365 nm UV irradiation. **(l)** Change in PL spectra of NTPAN-F in DCM (2.0 mM) at various conditions: the original solution (before 365 nm UV), the photochromic solution (after 365 nm UV irradiation) and the photochromic solution (placed naturally for 48 hours) respectively.

4. Supplementary Tables

Table S1. Crystallographic data of TPAN, TPAN-F, TPAN-Cl, TPAN-Br, TPAN-I.

source	TPAN	TPAN-F	TPAN-Cl	TPAN-Br	TPAN-I
CCDC	2054237	2054250	2054251	2054252	2054253
Formula	$C_{21}H_{15}N$	$C_{21}H_{14}FN$	$C_{21}H_{14}ClN$	$C_{21}H_{14}BrN$	$C_{21}H_{14}IN$
$D_{calc.}$/ g cm^{-3}	1.244	1.285	1.276	1.482	1.589
μ/mm^{-1}	0.072	0.083	0.231	2.544	14.747
Formula Weight	281.34	299.33	315.78	360.24	407.23
Colour	colourless	colourless	colourless	colourless	colourless
T/K	150(2)	150(2)	293(2)	150(2)	295(2)
Crystal System	monoclinic	triclinic	triclinic	triclinic	triclinic
Space Group	$P2_1/c$	P-1	P-1	P-1	P-1
a (Å)	9.8520(18)	8.4617(8)	9.509(9)	9.4954(9)	9.6674(4)
b (Å)	9.5451(16)	9.9195(9)	9.570(10)	9.5538(8)	9.7329(4)
c (Å)	16.504(2)	10.0112(10)	10.324(10)	10.1628(9)	10.2634(7)
α	90	106.884(5)	63.11(2)	63.011(4)	63.694(2)
β	104.615(5)	104.687(5)	79.79(2)	81.004(4)	81.390(3)
γ	90	91.445(5)	81.27(3)	80.806(4)	80.864(2)
volume (Å3)	1501.8(4)	773.36(13)	821.9(14)	807.29(13)	851.27(8)
Z	4	2	2	2	2
Z'	1	1	1	1	1
wavelength (Å)	0.71073	0.71073	0.71073	0.71073	1.54178
Radiation type	MoK_a	MoK_a	MoK_a	MoK_a	MoK_a
Θmin/°	2.486	2.158	2.229	2.183	4.651
Θmax/°	26.447	26.403	27.409	26.444	72.096
Measured Refl's.	24679	16287	15991	14512	8529
Ind't Refl's	3069	3176	3691	3303	3273
Refl's with I > 2(I)	1956	1873	1509	2619	3161
R_{int}	0.0875	0.1119	0.1668	0.0625	0.0591
Largest Peak	0.277	0.194	0.2	0.34	3.304
Deepest Hole	-0.19	-0.235	-0.231	-0.342	-3.59
GooF	1.037	1.032	1.03	1.045	1.207

wR_2	0.1223	0.1023	0.179	0.0855	0.2529
R_1	0.0558	0.0542	0.0786	0.0402	0.1053

Table S2. Crystallographic data of NTPAN, NTPAN-F, NTPAN-Cl, NTPAN-Br and NTPAN-I.

source	**NTPAN**	**NTPAN-F**	**NTPAN-Cl**	**NTPAN-Br**	**NTPAN-I (G-Type)**	**NTPAN-I (Y-Type)**
CCDC	2054256	2054258	2054257	2054254	2054255	2054898
Formula	$C_{25}H_{25}N_3$	$C_{25}H_{24}FN_3$	$C_{25}H_{24}ClN_3$	$C_{25}H_{24}BrN_3$	$C_{25}H_{24}IN_3$	$C_{25}H_{24}IN_3$
$D_{calc.}$/ g cm^{-3}	1.195	1.234	1.258	1.382	1.493	1.524
μ/mm^{-1}	0.071	0.08	0.196	1.931	1.474	1.505
Formula Weight	367.48	385.47	401.92	446.38	493.37	493.37
Colour	yellow	yellow	yellow	yellow	yellow	yellow
T/K	150	150(2)	150	150(2)	153(2)	153(2)
Crystal System	monoclinic	monoclinic	monoclinic	triclinic	triclinic	triclinic
Space Group	$P2_1/c$	$P2_1/c$	$P2_1/c$	P-1	P-1	P-1
a (Å)	10.4826(6)	10.6861(5)	11.0058(6)	9.8541(6)	9.9437(5)	9.2457(5)
b (Å)	21.4895(11)	21.3893(10)	21.0329(9)	10.6234(6)	10.8454(5)	10.2690(6)
c (Å)	9.9353(4)	10.0313(6)	10.2712(5)	11.7377(7)	11.7215(5)	12.5126(7)
α	90	90	90	102.009(3)	102.807(2)	79.213(3)
β	114.143(2)	115.138(2)	116.795(2)	94.363(3)	93.095(2)	71.430(2)
γ	90	90	90	114.749(2)	115.385(2)	73.837(3)
volume (Å3)	2042.31(18)	2075.67(19)	2122.32(18)	1072.89(11)	1097.58(9)	1075.28(11)
Z	4	4	4	2	2	2
Z'	1	1	1	1	1	1
wavelength (Å)	0.71073	0.71073	0.71073	0.71073	0.71073	0.71073
Radiation type	MoK_α	MoK_α	MoK_α	MoK_α	MoK_α	MoK_α
Θmin/°	2.331	2.105	1.936	2.189	2.3	2.391
Θmax/°	26.399	26.396	26.399	26.484	26.447	26.445
Measured Refl's.	54232	30047	43696	19279	27220	21031
Ind't Refl's	4185	4255	4338	4427	4518	4424
Refl's with I > 2(I)	3215	2666	3169	3674	3856	3633
R_{int}	0.0701	0.1138	0.0869	0.0357	0.0426	0.0396
Largest Peak	0.155	0.185	0.271	0.338	0.824	0.951
Deepest Hole	-0.196	-0.197	-0.339	-0.394	-0.718	-1.015
GooF	1.031	1.047	1.133	1.024	1.036	1.061

wR_2	0.0926	0.1037	0.1129	0.0784	0.067	0.0719
R_1	0.0396	0.0512	0.0429	0.0322	0.0295	0.0332

Table S3. Photophysical properties of TPAN, TPAN-F, TPAN-Cl, TPAN-Br, TPAN-I, NTPAN, NTPAN-F, NTPAN-Cl, NTPAN-Br and NTPAN-I in different states.

	λ_{ab} (nm)	λ_{em} (nm)	τ (ns)	Φ (%)	K_r (10^8 s^{-1})	K_{nr} (10^8 s^{-1})
TPAN	—	468	1.1	22.40	2.0	**7.1**
TPAN-F	—	467	0.7	10.94	1.6	12.7
TPAN-Cl	—	468	1.6	39.22	**2.5**	**3.8**
TPAN-Br	—	474	1.5	40.98	**2.7**	**3.9**
TPAN-I	—	475	1.3	49.79	**3.8**	**3.9**
NTPAN	—	571	3.1	33.08	1.1	2.2
NTPAN-F	—	541	2.1	27.42	1.3	3.5
NTPAN-Cl	—	566	3	73.10	2.4	0.9
NTPAN-Br	—	524	1.8	40.27	2.2	3.3
NTPAN-I	—	519	0.9	8.69	1.0	10.1
		Dispersed in Adamantane				
TPAN	—	445	1.2	18.80	**1.6**	**6.8**
TPAN-F	—	465	1.0	8.89	0.9	9.1
TPAN-Cl	—	474	1.6	26.17	**1.6**	**4.6**
TPAN-Br	—	477	1.7	35.99	**2.1**	**3.8**
TPAN-I	—	468	1.4	24.68	**1.8**	**5.4**
NTPAN	—	590	4.8	4.67	0.1	2.0
NTPAN-F	—	542	1.7	8.23	0.48	5.4
NTPAN-Cl	—	575	2.7	29.00	1.1	2.6
NTPAN-Br	—	520	1.4	16.38	1.2	6.0
NTPAN-I	—	561	1	5.06	0.5	9.4
			In Solution			
TPAN	235/311	420	—	< 1	—	—
TPAN-F	238/312	440	—	< 1	—	—
TPAN-Cl	240/312	492	—	< 1	—	—
TPAN-Br	246/312	451	—	< 1	—	—
TPAN-I	246/312	471	—	< 1	—	—
NTPAN	257/374	571	—	< 1	—	—
NTPAN-F	229/377	541	—	< 1	—	—
NTPAN-Cl	262/383	575	—	< 1	—	—
NTPAN-Br	269/383	520	—	< 1	—	—
NTPAN-I	269/386	500	—	< 1	—	—

Table S4. Contribution ratioes of different atoms to HOMOs and LUMOs of TPAN, TPAN-F, TPAN-Cl, TPAN-Br and TPAN-I

Compound	Group	Contribution to HOMO (%)	Contribution to LUMO (%)
TPAN	*Phenyl*	66.84	44.76
	Acrylonitrile	32.56	51.92
TPAN-F	*Phenyl*	66.06	43.73
	Acrylonitrile	31.11	52.61
	F	2.26	0.45
TPAN-Cl	*Phenyl*	64.22	45.00
	Acrylonitrile	29.77	51.11
	Cl	5.45	0.66
TPAN-Br	*Phenyl*	62.78	45.04
	Acrylonitrile	29.12	51.21
	Br	7.60	0.59
TPAN-I	*Phenyl*	59.04	45.21
	Acrylonitrile	25.75	51.00
	I	14.73	0.62

Table S5. Contribution ratioes of different atoms to HOMOs and LUMOs of NTPAN, NTPAN-F, NTPAN-Cl, NTPAN-Br and NTPAN-I

Compound	Center	Contribution to HOMO (%)	Contribution to LUMO (%)
NTPAN	*Phenyl*	51.75	42.47
	Acrylonitrile	21.27	49.60
	Dimethylamino	26.04	4.61
NTPAN-F	*Phenyl*	51.93	40.65
	Acrylonitrile	21.00	50.14
	Dimethylamino	26.00	4.74
	F	0.67	0.48
NTPAN-Cl	*Phenyl*	50.90	43.33
	Acrylonitrile	20.97	47.97
	Dimethylamino	25.90	4.69
	Cl	1.24	0.67
NTPAN-Br	*Phenyl*	50.65	43.30
	Acrylonitrile	20.91	48.17
	Dimethylamino	26.10	4.72
	Br	1.38	0.59
NTPAN-I	*Phenyl*	50.51	43.54
	Acrylonitrile	20.83	47.89

Dimethylamino	25.71	4.70
I	1.95	0.63

Table S6. Excitation energies of first 10 states for TPAN, TPAN-F, TPAN-Cl, TPAN-Br and TPAN-I calculated with TDDFT at PBE0/6-311+G(d,p) level.

State No	TPAN	TPAN-F	TPAN-Cl	TPAN-Br	TPAN-I
1	2.2949 eV (T_1)	2.2903 eV (T_1)	2.2704 eV (T_1)	2.2756 eV (T_1)	2.2693 eV (T_1)
2	3.3783 eV (T_2)	3.3780 eV (T_2)	3.3660 eV (T_2)	3.3725 eV (T_2)	3.3477 eV (T_2)
3	3.4438 eV (T_3)	**3.4509 eV (T_3)**	**3.3745 eV (T_3)**	**3.3770 eV (T_3)**	**3.3738 eV (T_3)**
4	**3.5951 eV (T_4)**	**3.6991 eV (S_1)**	**3.6680 eV (S_1)**	**3.6658 eV (S_1)**	**3.6232 eV (S_1)**
5	**3.7382 eV (S_1)**	3.7170 eV (T_4)	3.6847 eV (T_4)	3.6858 eV (T_4)	3.6828 eV (T_4)
6	4.0377 eV (T_5)	4.0241 eV (T_5)	3.9971 eV (T_5)	3.9911 eV (T_5)	3.9914 eV (T_5)
7	4.0703 eV (T_6)	4.0981 eV (T_6)	4.0775 eV (T_6)	4.0760 eV (T_6)	4.0126 eV (T_6)
8	4.1798 eV (T_7)	4.1625 eV (T_7)	4.1655 eV (T_7)	4.1648 eV (T_7)	4.0687 eV (T_7)
9	4.3431 eV (T_8)	4.3517 eV (T_8)	4.3099 eV (T_8)	4.3014 eV (T_8)	4.1346 eV (T_8)
10	4.4116 eV (T_9)	4.4036 eV (T_9)	4.3713 eV (T_9)	4.3597 eV (T_9)	4.2373 eV (T_9)

Table S7. Excitation energies of first 10 states for NTPAN, NTPAN-F, NTPAN-Cl, NTPAN-Br and NTPAN-I calculated with TDDFT at PBE0/6-311+G(d,p) level.

State No	NTPAN	NTPAN-F	NTPAN-Cl	NTPAN-Br	NTPAN-I
1	2.0974 eV (T_1)	2.0831 eV (T_1)	2.0643 eV (T_1)	2.0704 eV (T_1)	2.0678 eV (T_1)
2	**2.9221 eV (T_2)**	**2.9068 eV (T_2)**	**2.8773 eV (T_2)**	**2.8724 eV (T_2)**	**2.8718 eV (T_2)**
3	**3.2207 eV (S_1)**	**3.2039 eV (S_1)**	**3.1533 eV (S_1)**	**3.1531 eV (S_1)**	**3.1416 eV (S_1)**
4	3.3261 eV (T_3)	3.3222 eV (T_3)	3.2545 eV (T_3)	3.2644 eV (T_3)	3.2473 eV (T_3)
5	3.4940 eV (S_2)	3.4772 eV (S_2)	3.4304 eV (S_2)	3.4236 eV (S_1)	3.4218 eV (S_2)
6	3.5325 eV (T_4)	3.5165 eV (T_4)	3.5044 eV (T_4)	3.5047 eV (T_4)	3.5023 eV (T_4)
7	3.6206 eV (T_5)	3.6159 eV (T_5)	3.5875 eV (T_5)	3.5912 eV (T_5)	3.5886 eV (T_5)
8	3.6901 eV (T_6)	3.6791 eV (T_6)	3.6773 eV (T_6)	3.6783 eV (T_6)	3.6775 eV (T_6)
9	3.8135 eV (T_7)	3.8037 eV (T_7)	3.7899 eV (T_7)	3.7866 eV (T_7)	3.7842 eV (T_7)
10	3.9050 eV (T_8)	3.8868 eV (T_8)	3.8693 eV (T_8)	3.8684 eV (T_8)	3.8142 eV (T_8)

Table S8. Experimental and calculated S_0->S_1 absorption wavelengths of TPAN compounds and their cyclized products in DCM

Compounds	λ_{exp} (nm)	λ_{cal} (nm)
TPAN	311	341
TPAN cyclized product	477	557
TPAN-F	312	345
TPAN-F cyclized product	483	556
TPAN-Cl	312	350
TPAN-Cl cyclized product	486	556
TPAN-Br	312	355
TPAN-Br cyclized product	487	554
TPAN-I	312	356
TPAN-I cyclized product	486	553

Table S9. Experimental and calculated S_0->S_1 absorption wavelengths of NTPAN compounds, their cyclized products and dehydrogenated products in DCM

Compounds	λ_{exp} (nm)	λ_{cal} (nm)
NTPAN	374	440
NTPAN cyclized product	630	733
NTPAN dehydrogenated product	523	573
NTPAN-F	377	439
NTPAN-F cyclized product	630	633
NTPAN-F dehydrogenated product	523	591
NTPAN-Cl	383	444
NTPAN-Cl cyclized product	628	683
NTPAN-Cl dehydrogenated product	525	592
NTPAN-Br	383	447
NTPAN-Br cyclized product	628	685
NTPAN-Br dehydrogenated product	525	591
NTPAN-I	386	448
NTPAN-I cyclized product	628	685
NTPAN-I dehydrogenated product	526	590

5. NMR and HRMS Spectra of Compounds

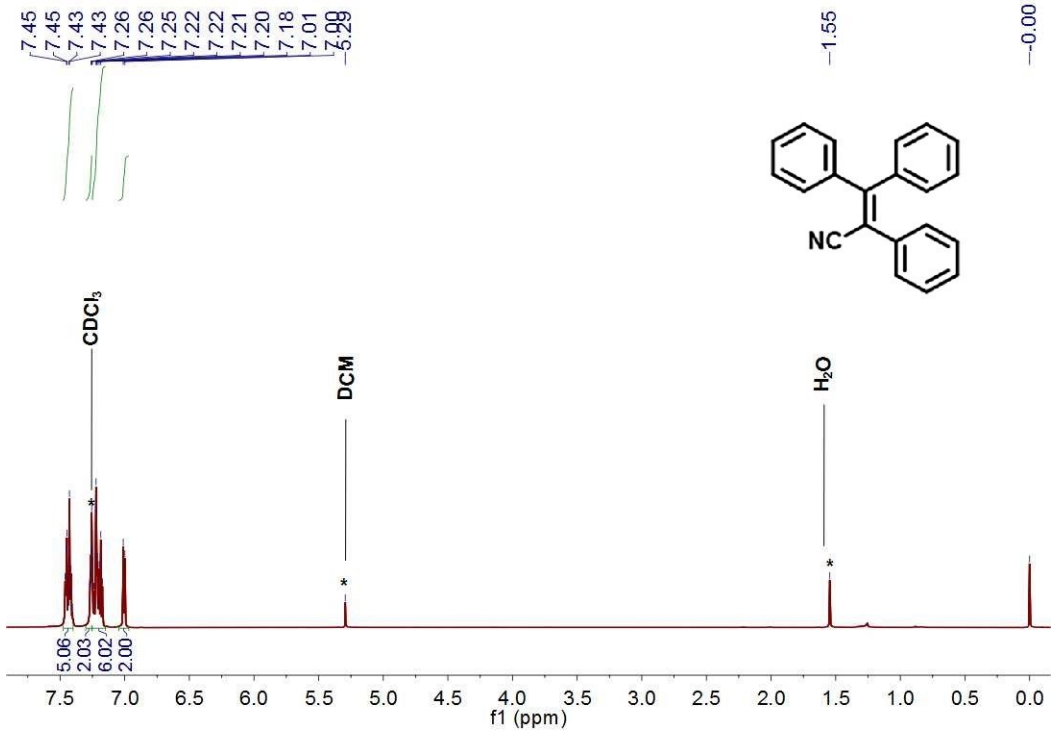

^{1}H NMR spectrum of 2,3,3-triphenylacrylonitrile (TPAN) in $CDCl_3$

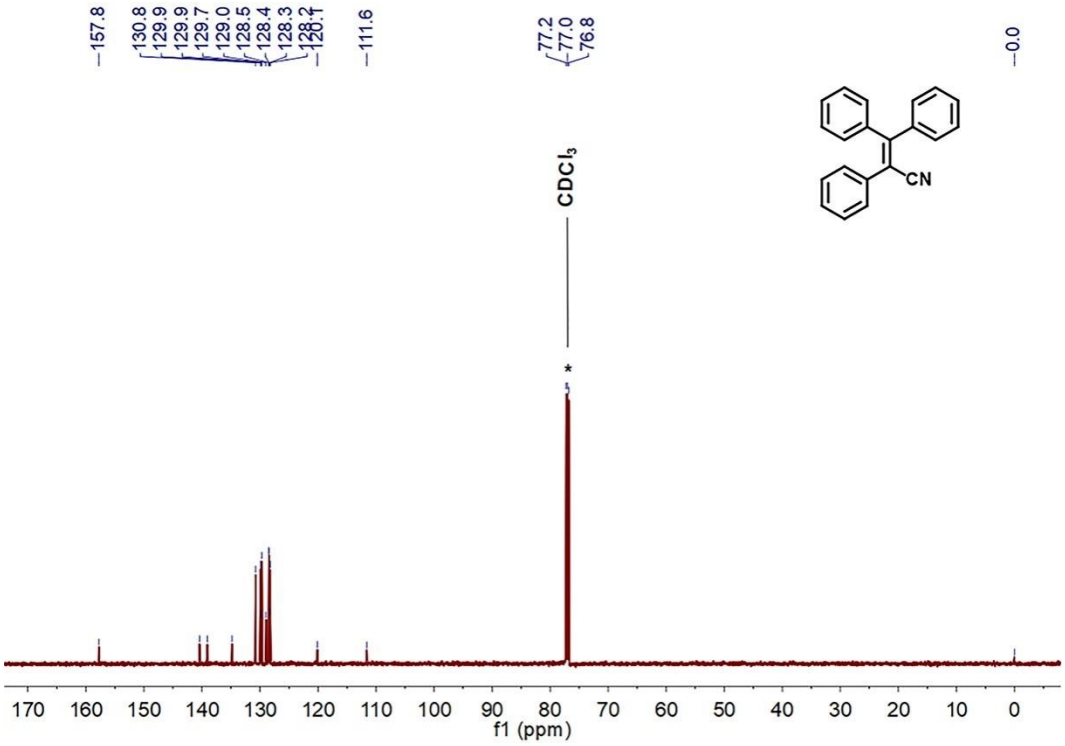

^{13}C NMR spectrum of 2,3,3-triphenylacrylonitrile (TPAN) in $CDCl_3$

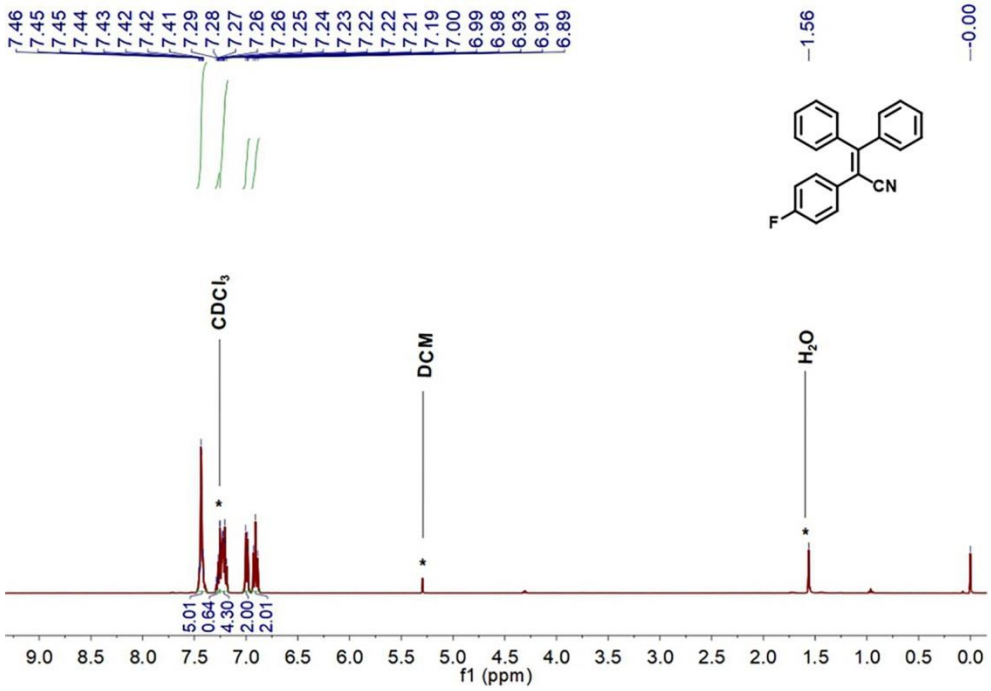

^{1}H NMR spectrum of 2-(4-fluorophenyl)-3,3-diphenylacrylonitrile(TPAN-F) in $CDCl_3$

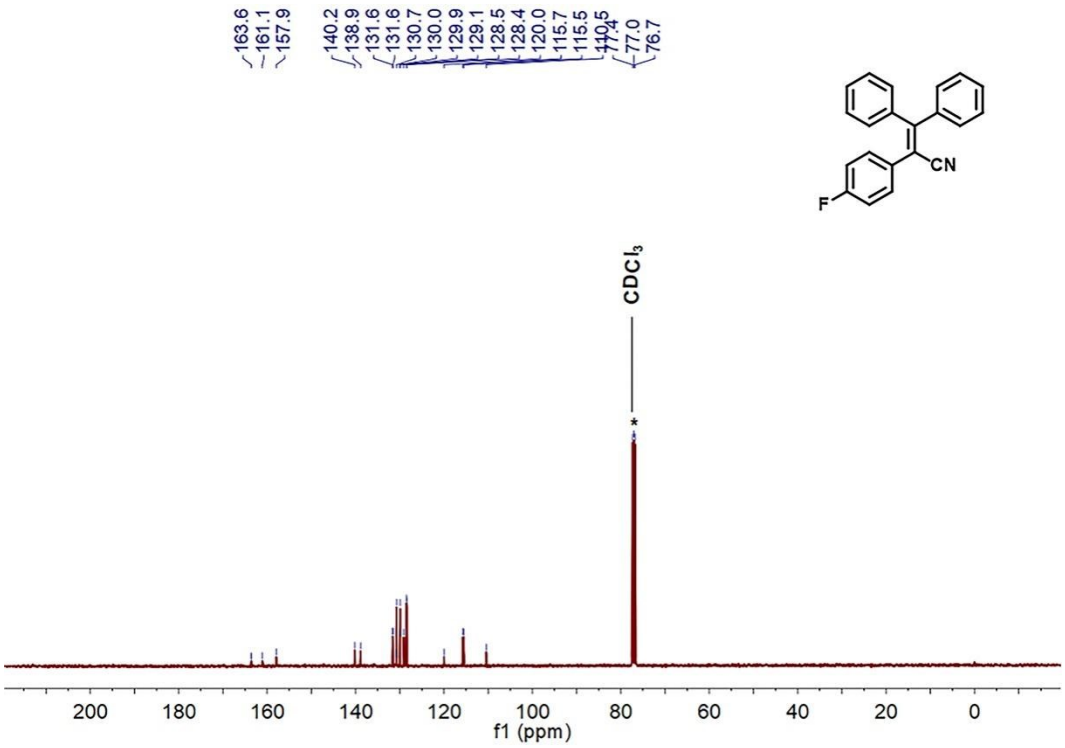

^{13}C NMR spectrum of 2-(4-fluorophenyl)-3,3-diphenylacrylonitrile(TPAN-F) in $CDCl_3$

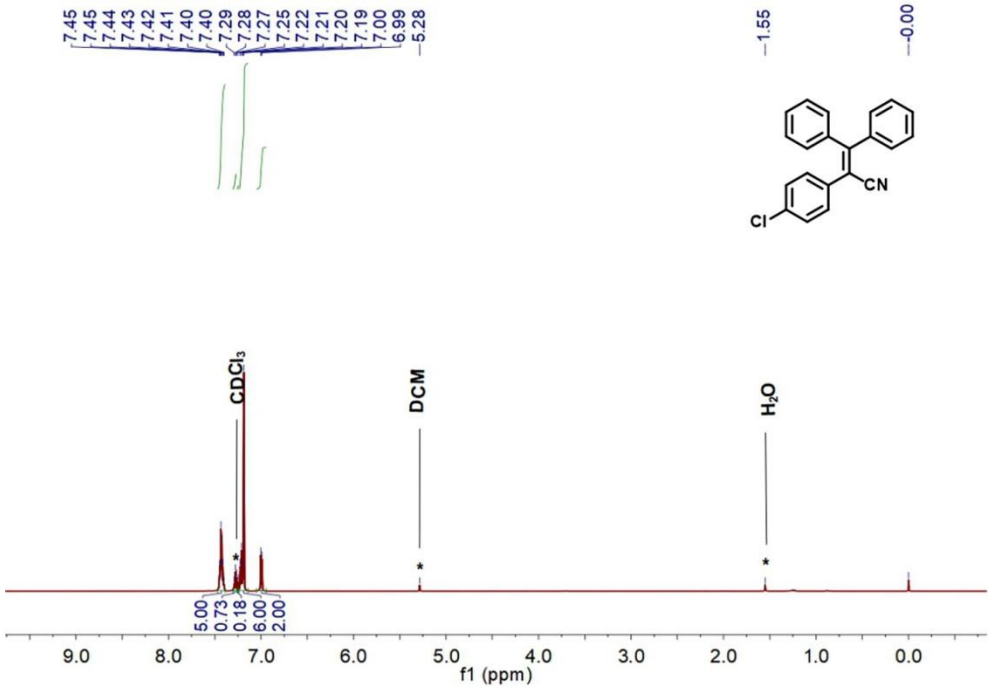

^{1}H NMR spectrum of 2-(4-chlorophenyl)-3,3-diphenylacrylonitrile (TPAN-Cl) in $CDCl_3$

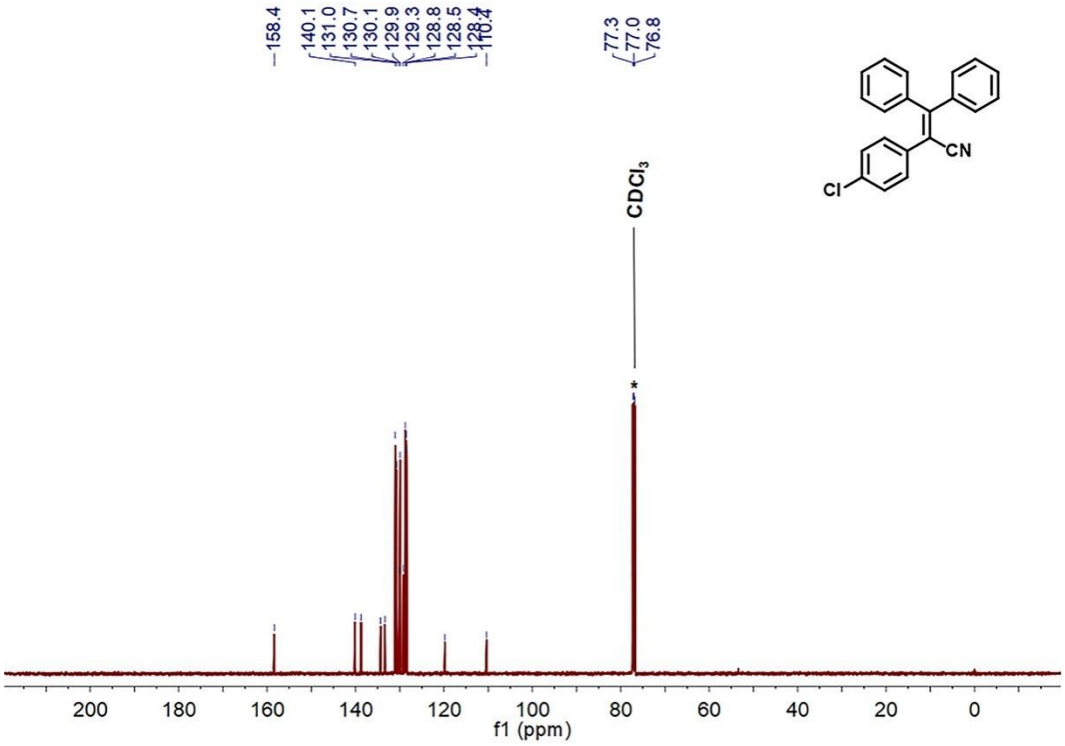

^{13}C NMR spectrum of 2-(4-chlorophenyl)-3,3-diphenylacrylonitrile (TPAN-Cl) in $CDCl_3$

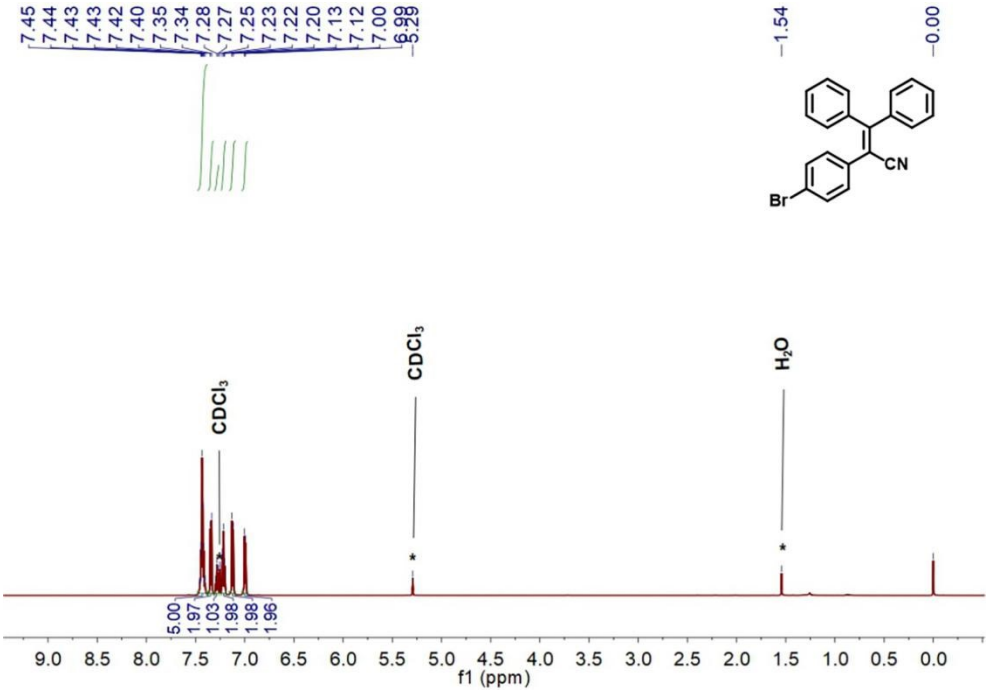

^{1}H NMR spectrum of 2-(4-bromophenyl)-3,3-diphenylacrylonitrile(TPAN-Br) in $CDCl_3$

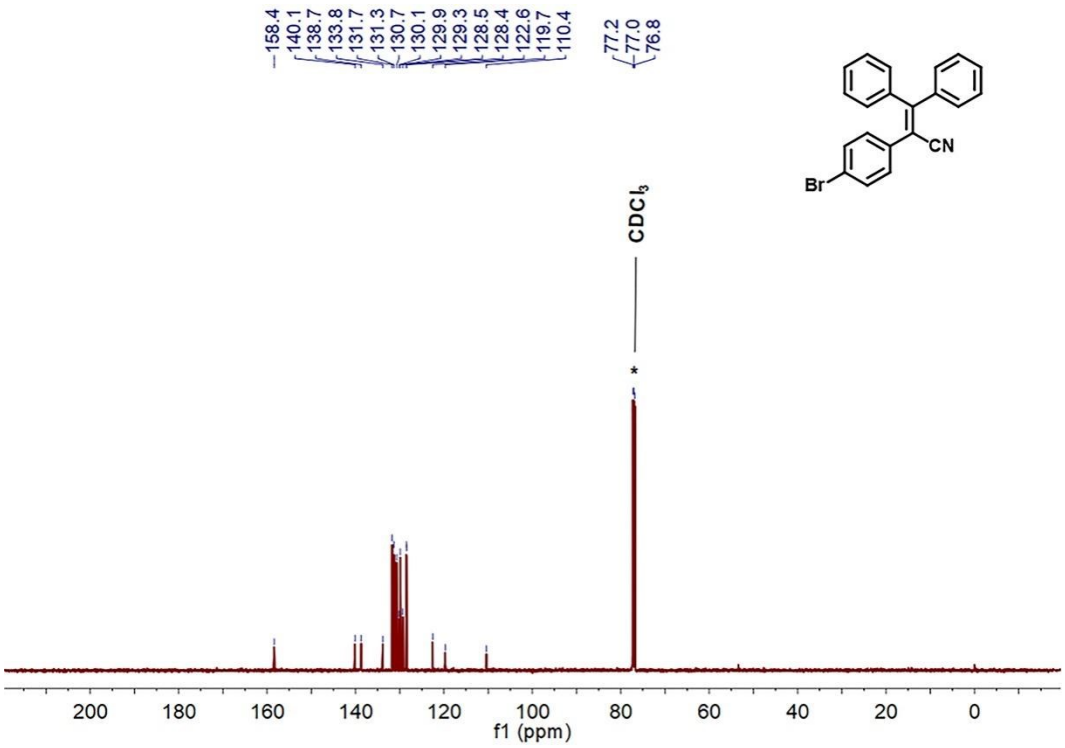

^{13}C NMR spectrum of 2-(4-bromophenyl)-3,3-diphenylacrylonitrile(TPAN-Br) in $CDCl_3$

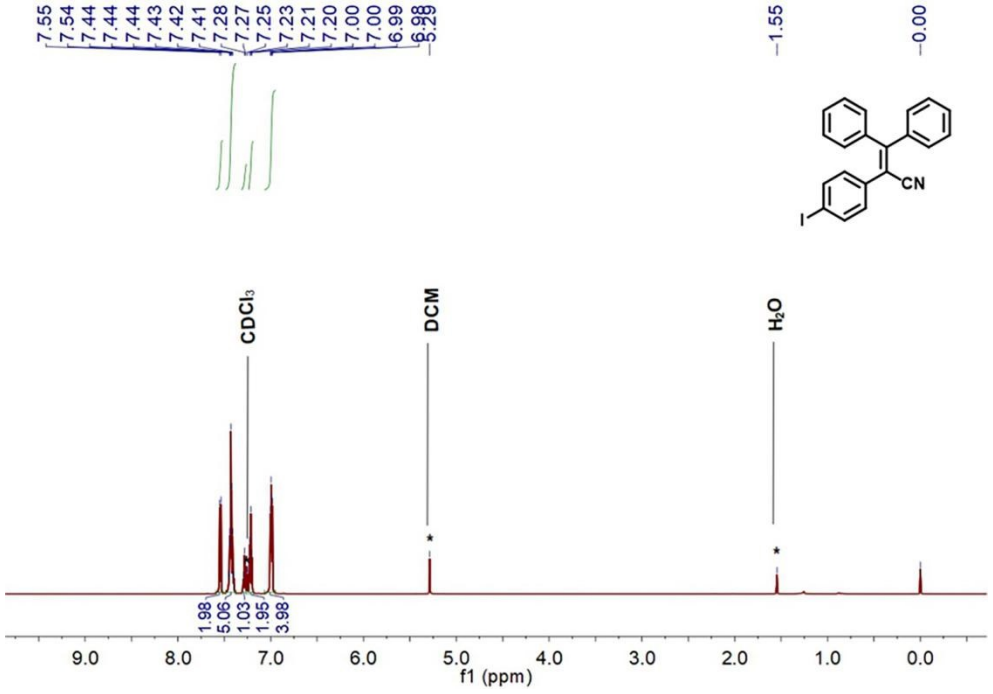

^{1}H NMR spectrum of 2-(4-iodophenyl)-3,3-diphenylacrylonitrile(TPAN-I) in $CDCl_3$

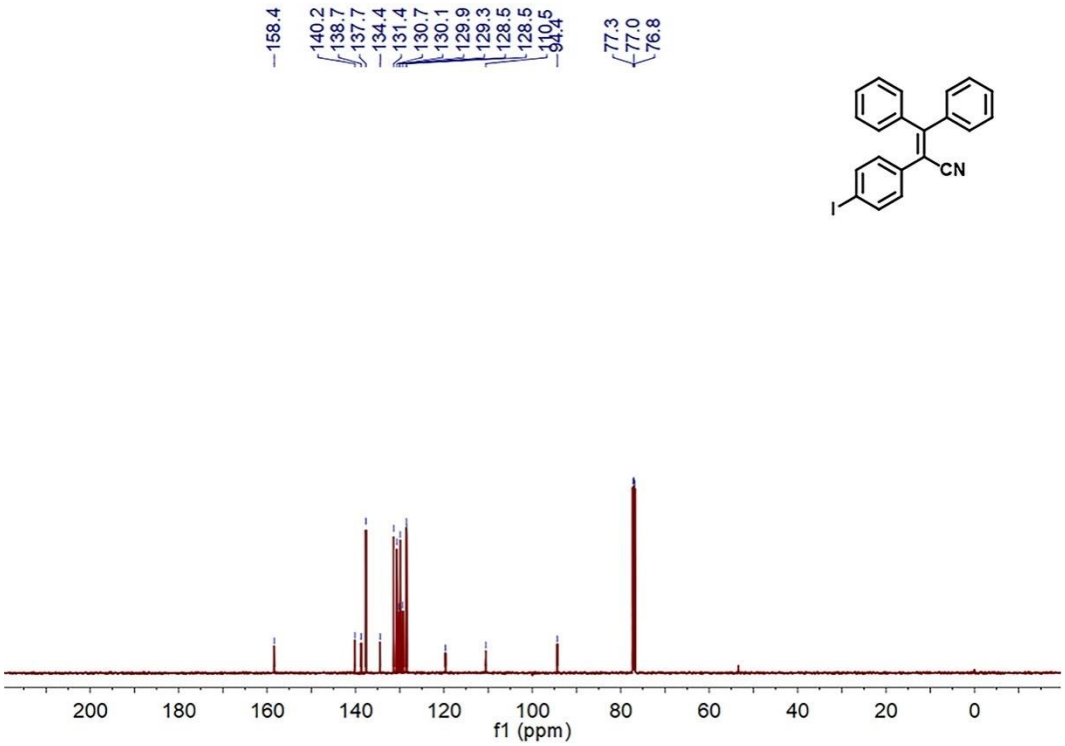

^{13}C NMR spectrum of 2-(4-iodophenyl)-3,3-diphenylacrylonitrile(TPAN-I) in $CDCl_3$

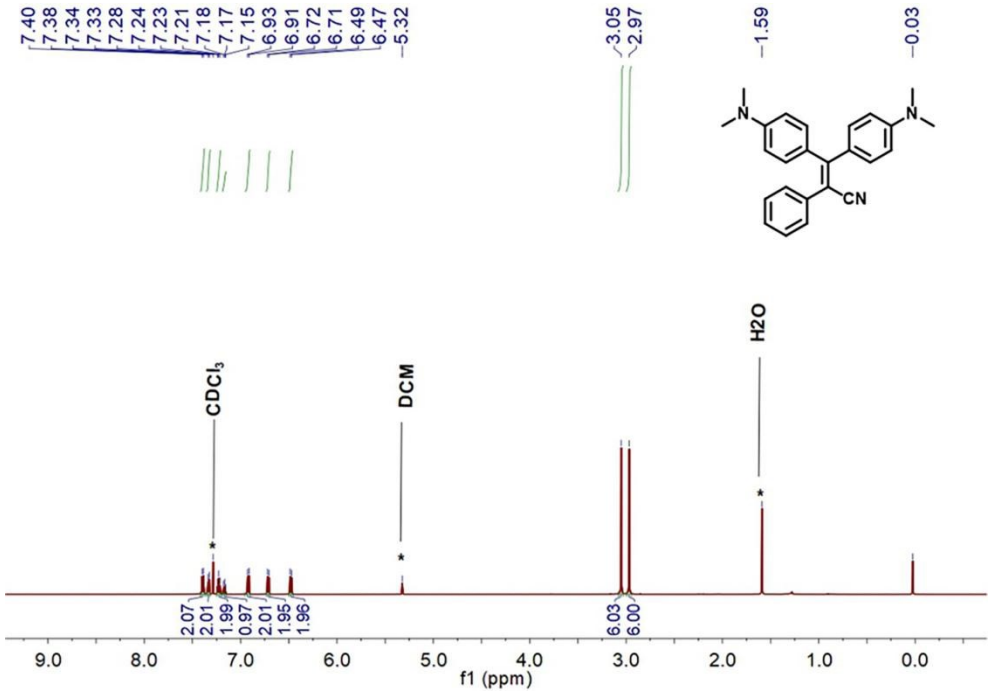

^{1}H NMR spectrum of 3,3-bis(4-(dimethylamino)phenyl)-2-phenylacrylonitrile (NTPAN) in $CDCl_3$

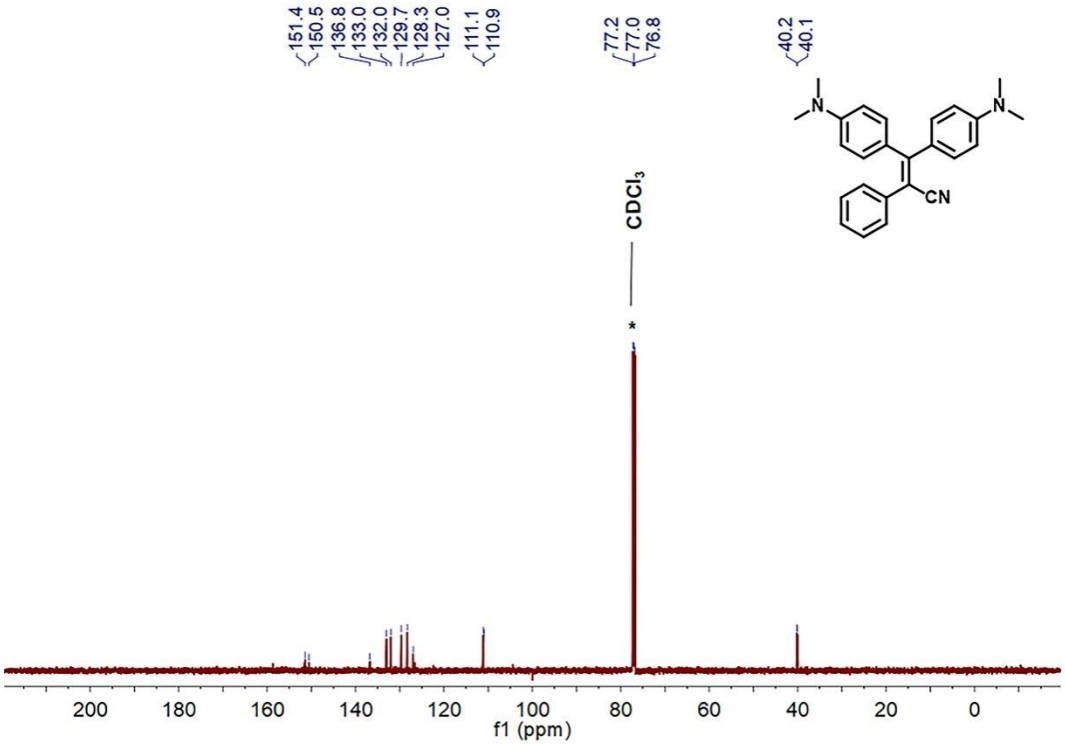

^{13}C NMR spectrum of 3,3-bis(4-(dimethylamino)phenyl)-2-phenylacrylonitrile (NTPAN) in $CDCl_3$

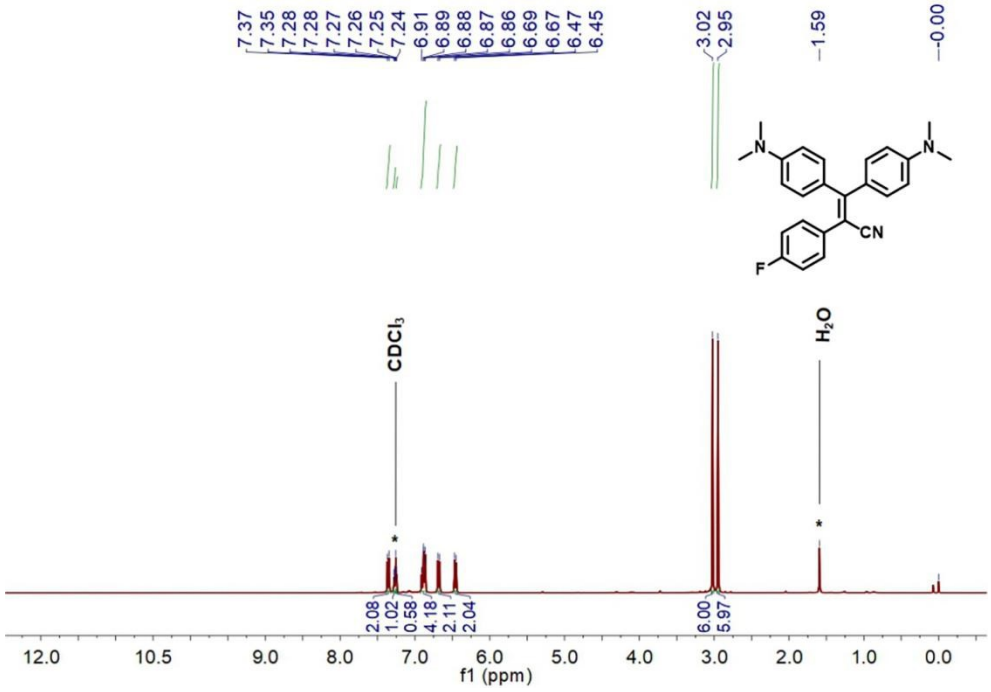

^{1}H NMR spectrum of 3,3-bis(4-(dimethylamino)phenyl)-2-(4-fluorophenyl) acrylonitrile(NTPAN-F) in $CDCl_3$

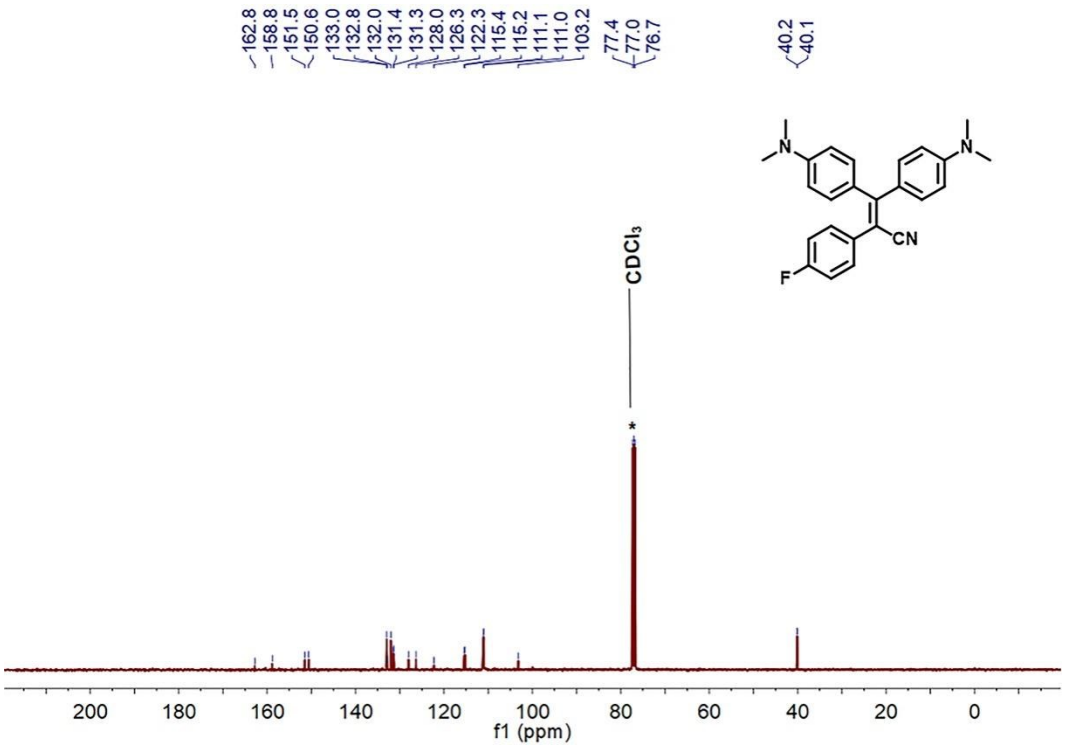

^{13}C NMR spectrum of 3,3-bis(4-(dimethylamino)phenyl)-2-(4-fluorophenyl) acrylonitrile(NTPAN-F) in $CDCl_3$

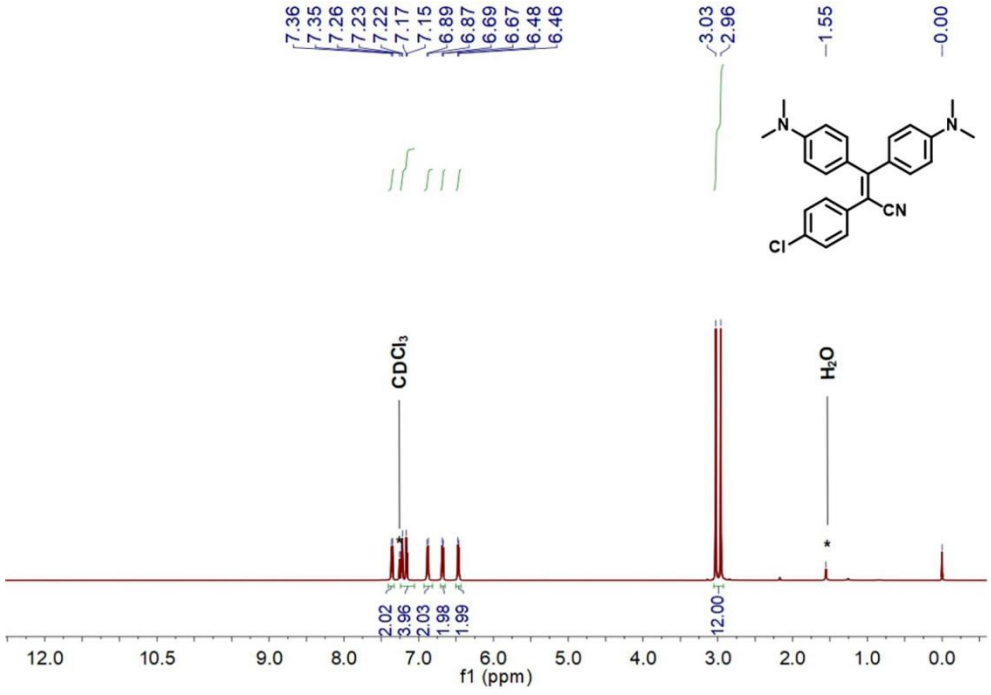

^{1}H NMR spectrum of 2-(4-chlorophenyl)-3,3-bis(4-(dimethylamino)phenyl) acrylonitrile(NTPAN-Cl) in $CDCl_3$

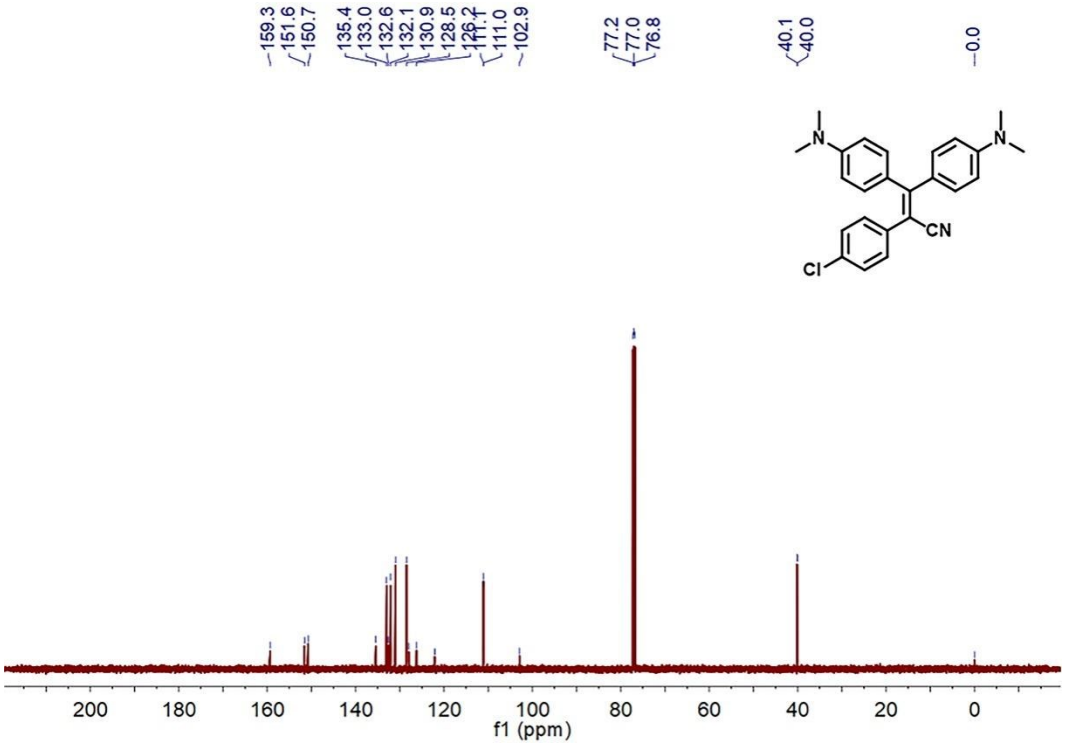

^{13}C NMR spectrum of 2-(4-chlorophenyl)-3,3-bis(4-(dimethylamino)phenyl) acrylonitrile(NTPAN-Cl) in $CDCl_3$

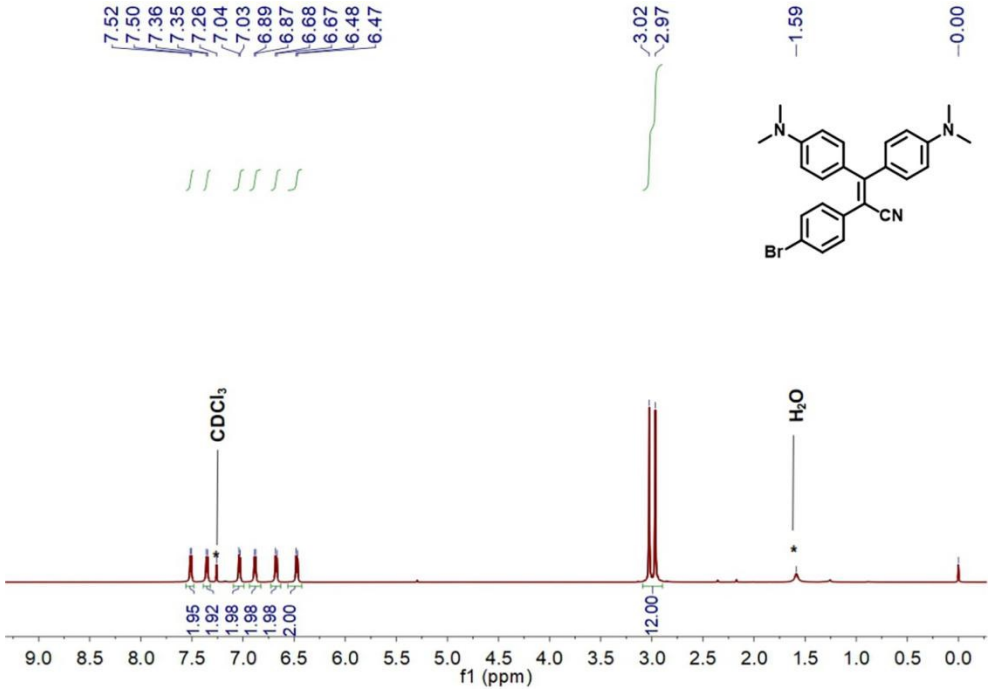

^{1}H NMR spectrum of 2-(4-bromophenyl)-3,3-bis(4-(dimethylamino)phenyl) acrylonitrile(NTPAN-Br) in $CDCl_3$

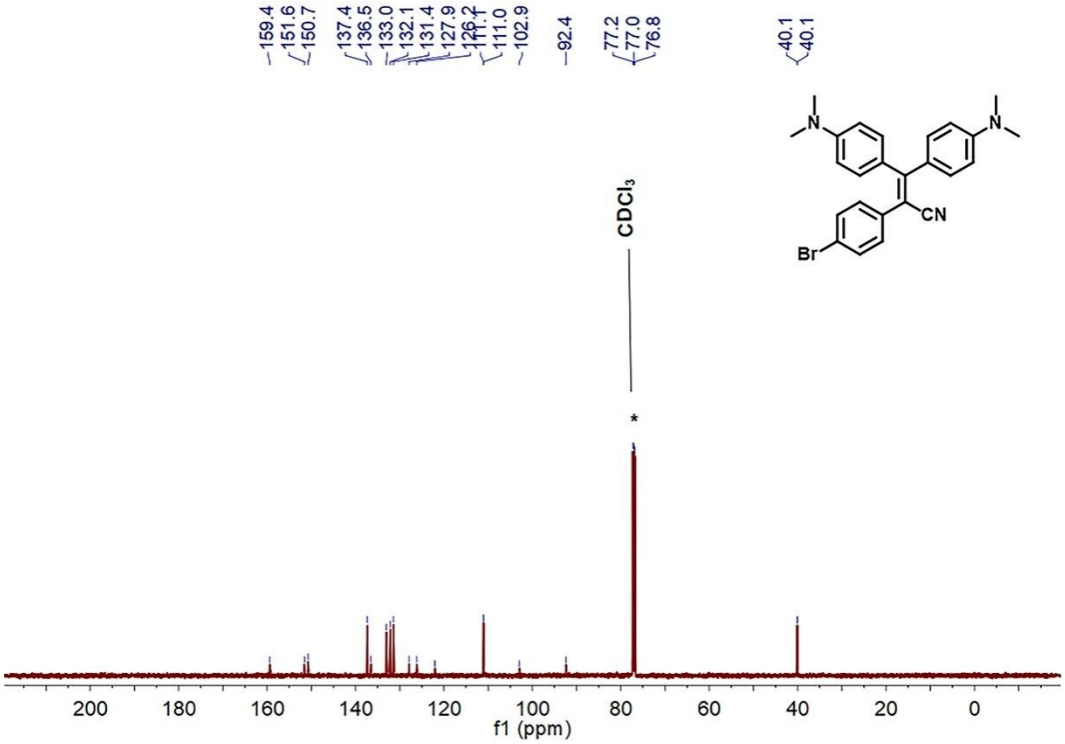

^{13}C NMR spectrum of 2-(4-bromophenyl)-3,3-bis(4-(dimethylamino)phenyl) acrylonitrile(NTPAN-Br) in $CDCl_3$

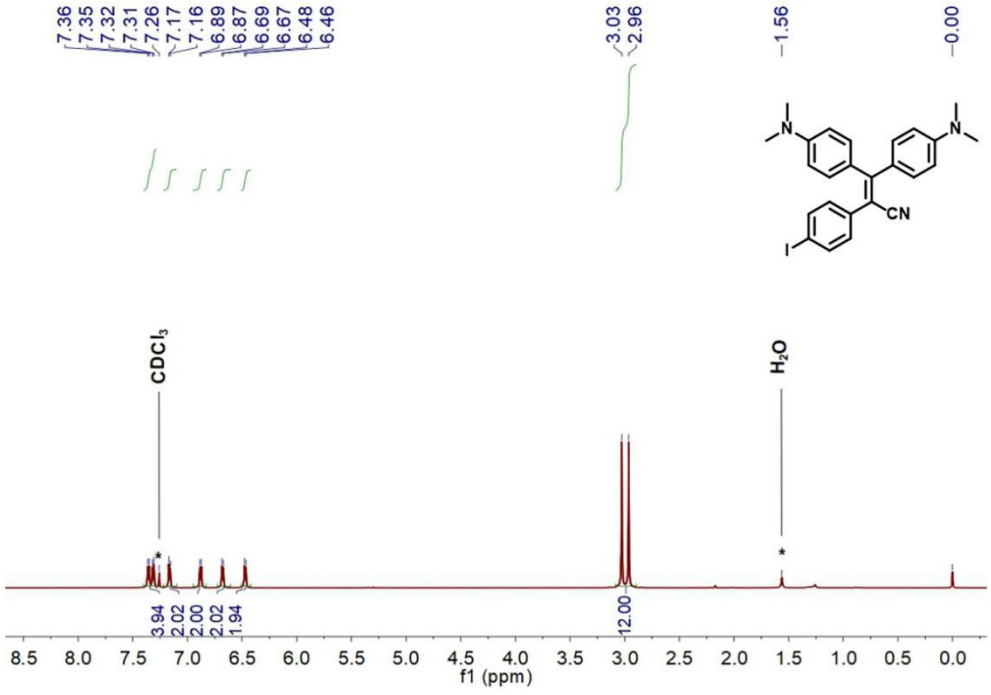

^{1}H NMR spectrum of 3,3-bis(4-(dimethylamino)phenyl)-2-(4-iodophenyl)acrylonitrile (NTPAN-I) in $CDCl_3$

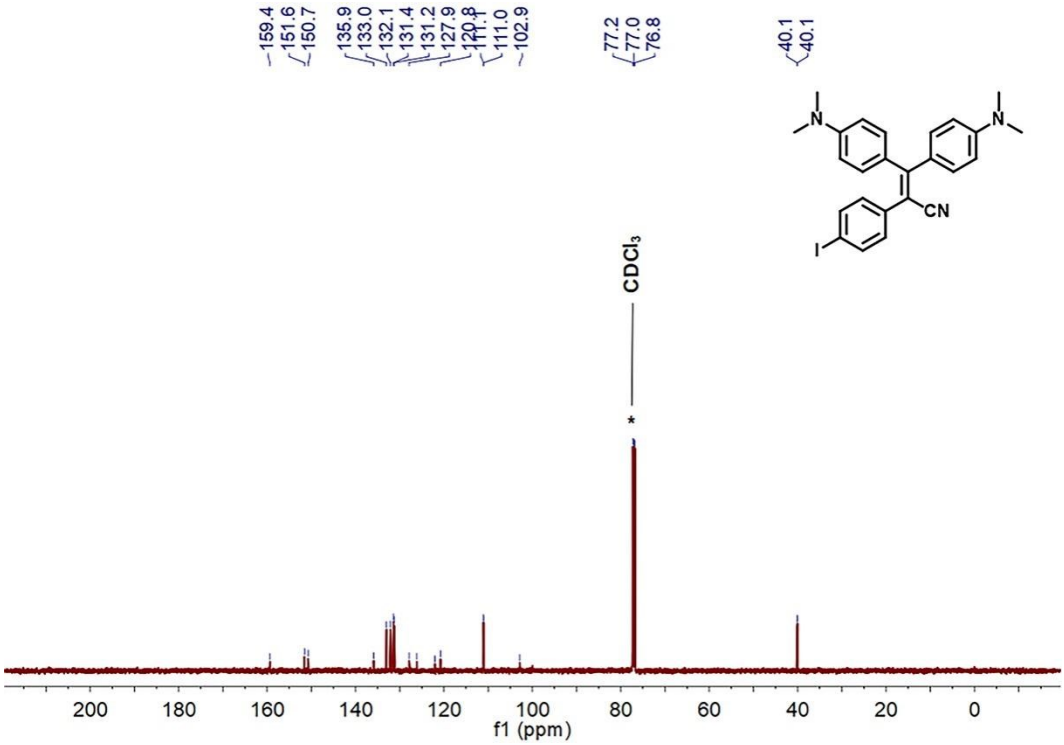

^{13}C NMR spectrum of 3,3-bis(4-(dimethylamino)phenyl)-2-(4-iodophenyl) acrylonitrile(NTPAN-I) in $CDCl_3$

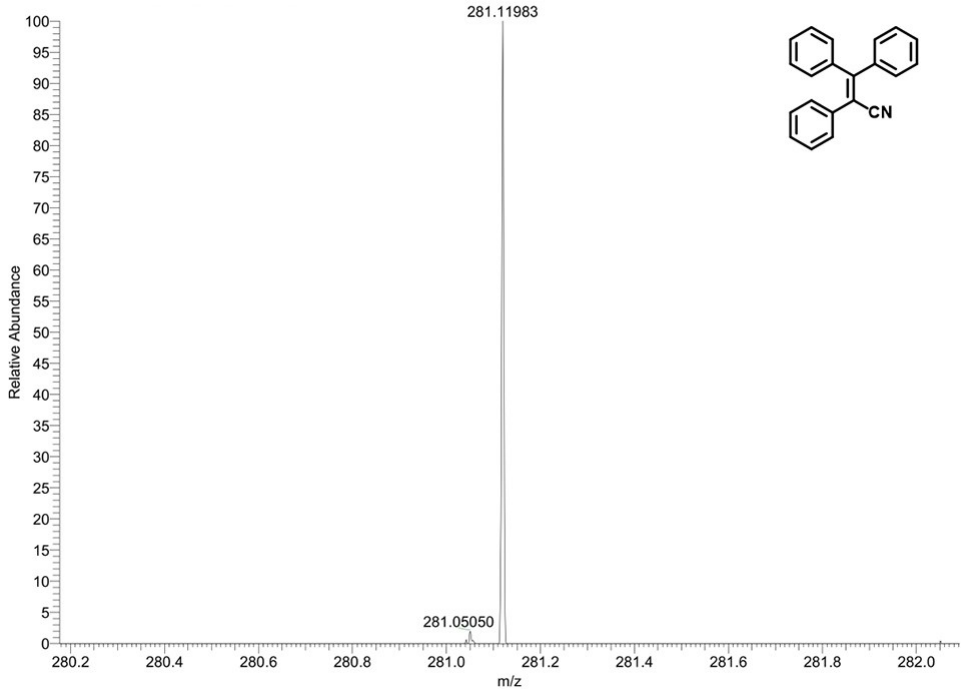

High-resolution mass spectrum of 2,3,3-triphenylacrylonitrile (TPAN)

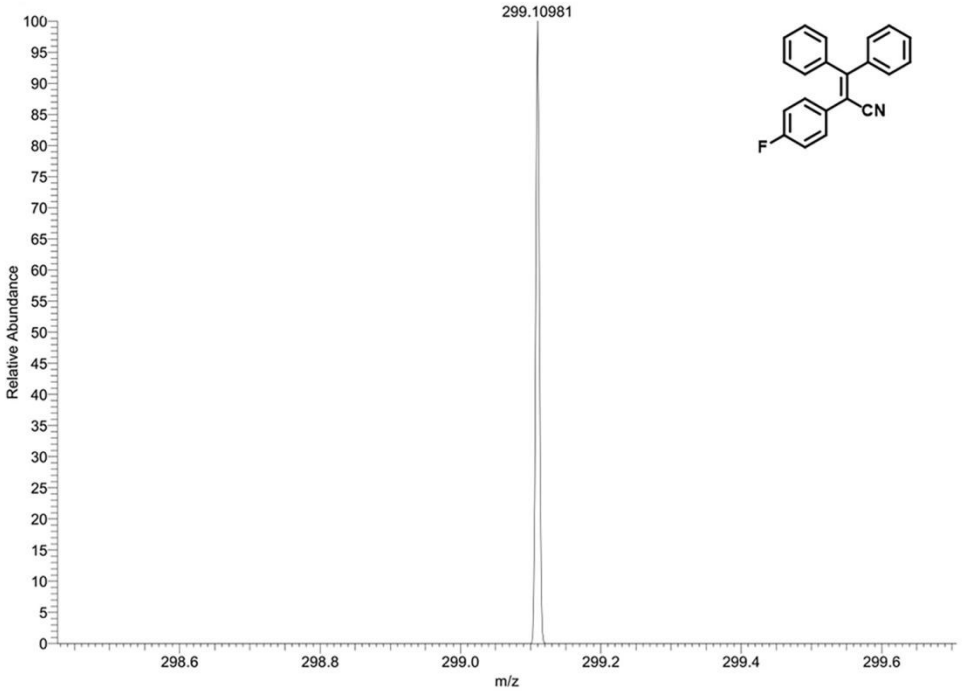

High-resolution mass spectrum of 2-(4-fluorophenyl)-3,3-diphenylacrylonitrile (TPAN-F)

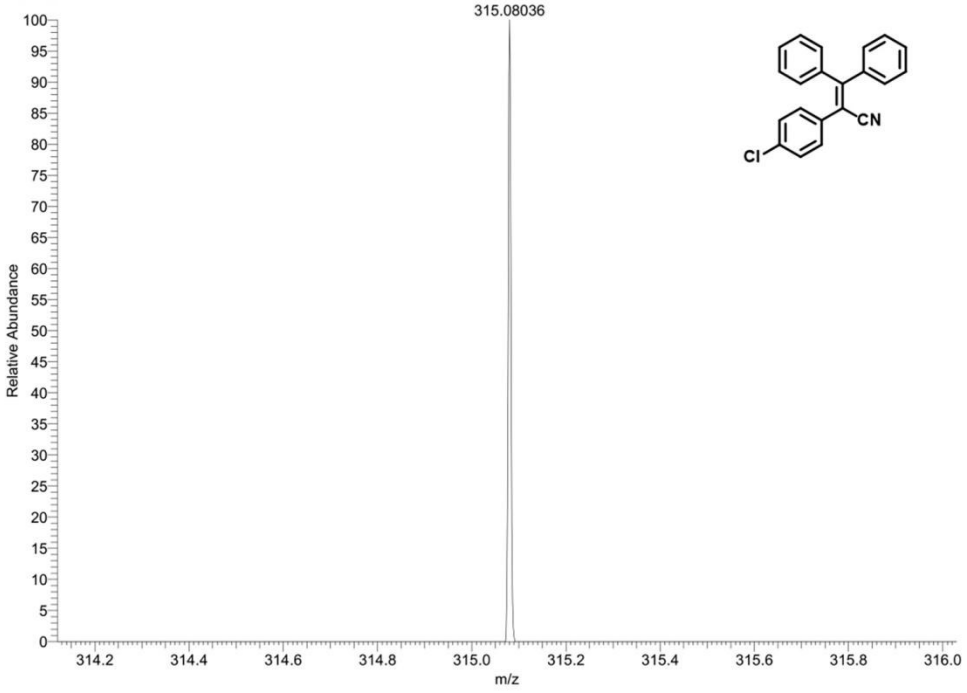

High-resolution mass spectrum of 2-(4-chlorophenyl)-3,3-diphenylacrylonitrile (TPAN-Cl)

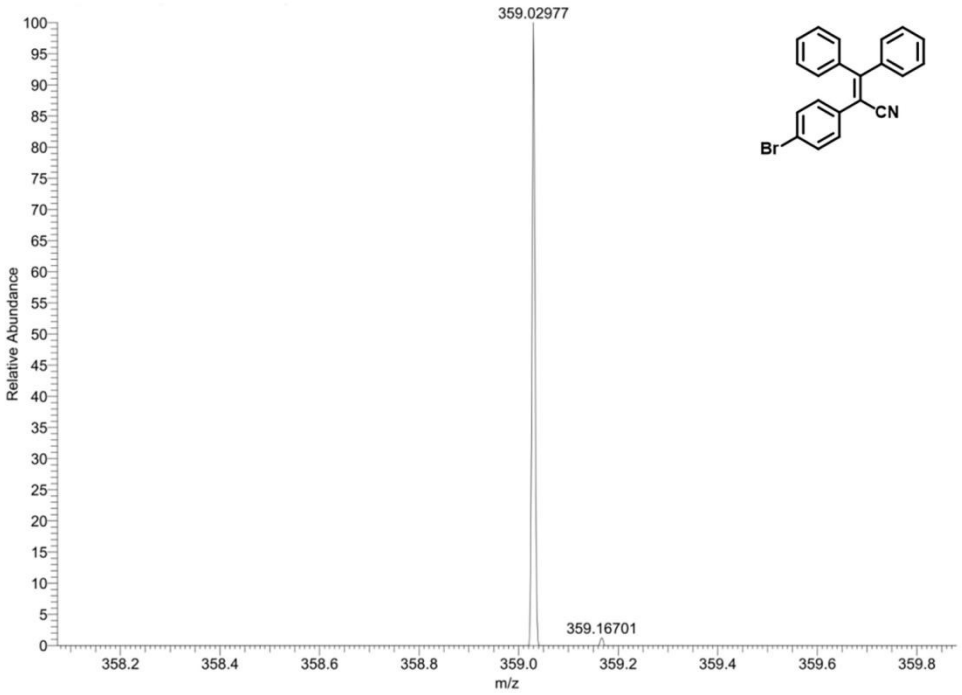

High-resolution mass spectrum of 2-(4-bromophenyl)-3,3-diphenylacrylonitrile (TPAN-Br)

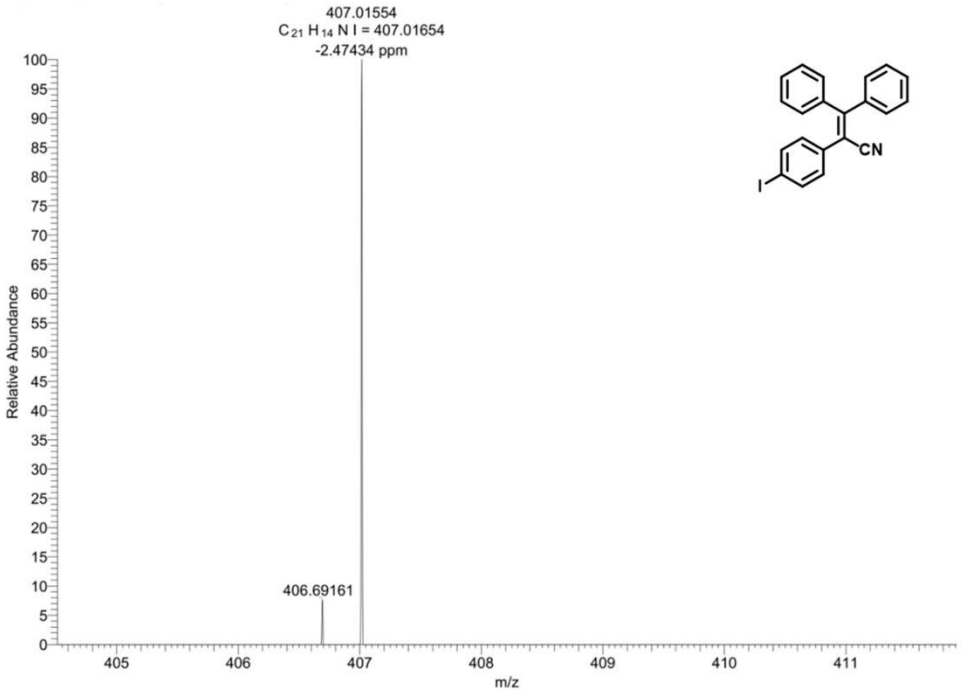

High-resolution mass spectrum of 2-(4-iodophenyl)-3,3-diphenylacrylonitrile (TPAN-I)

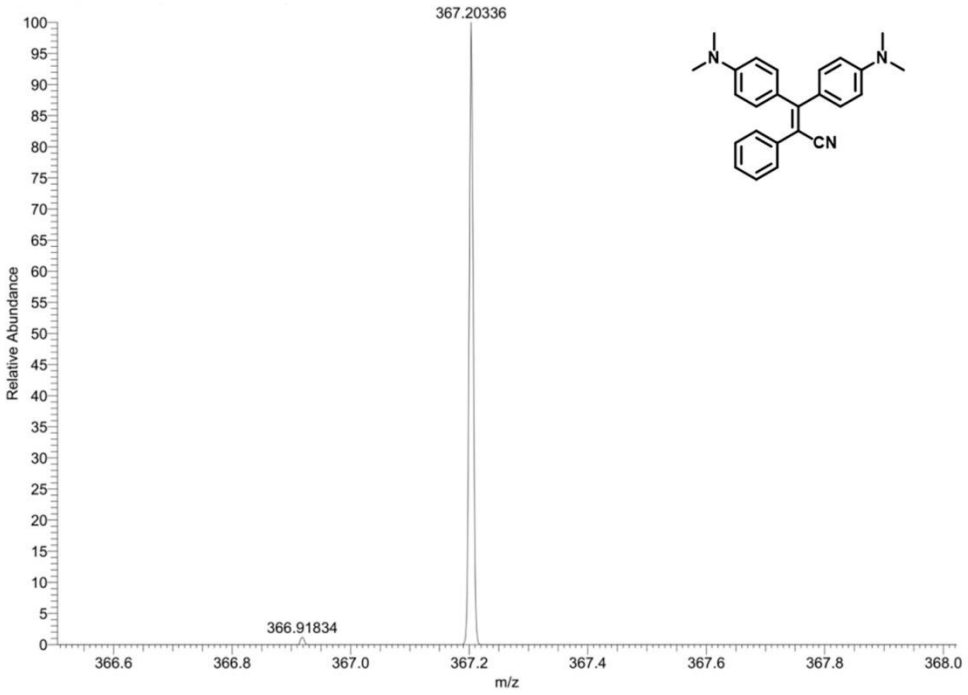

High-resolution mass spectrum of 3,3-bis(4-(dimethylamino)phenyl)-2-phenylacrylonitrile(NTPAN)

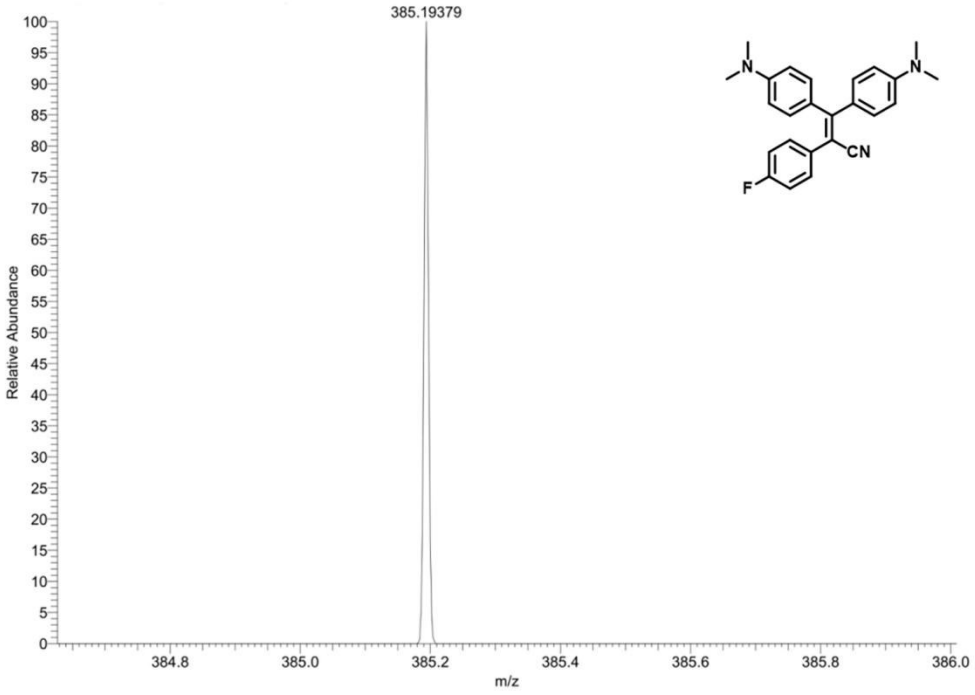

High-resolution mass spectrum of 3,3-bis(4-(dimethylamino)phenyl)-2-(4-fluorophenyl) acrylonitrile(NTPAN-F)

High-resolution mass spectrum of 2-(4-chlorophenyl)-3,3-bis(4-(dimethylamino) phenyl)acrylonitrile(NTPAN-Cl)

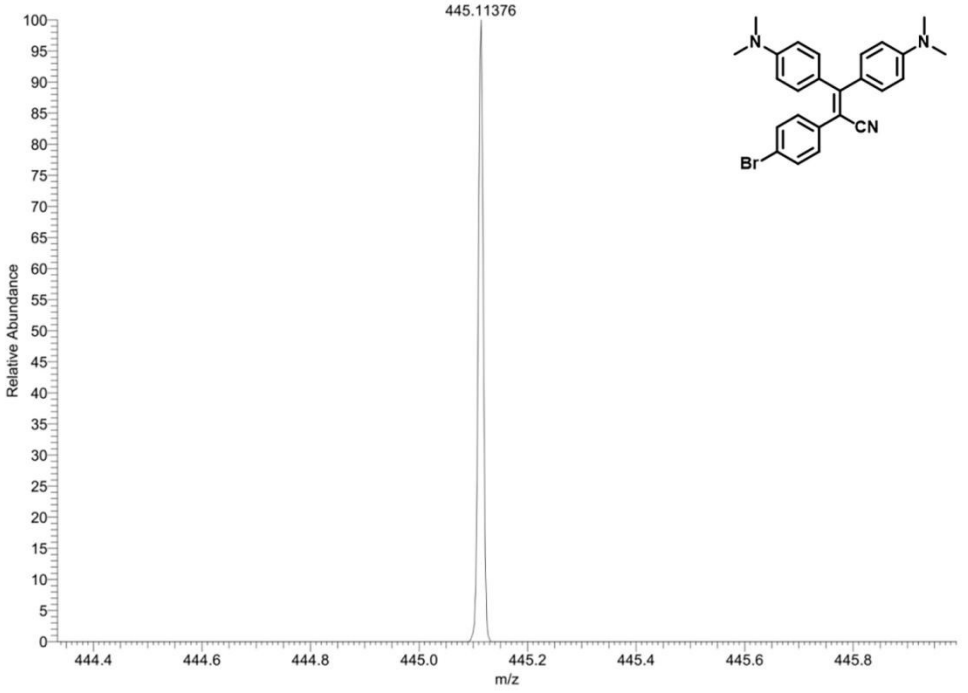

High-resolution mass spectrum of 2-(4-bromophenyl)-3,3-bis(4-(dimethylamino) phenyl)acrylonitrile(NTPAN-Br)

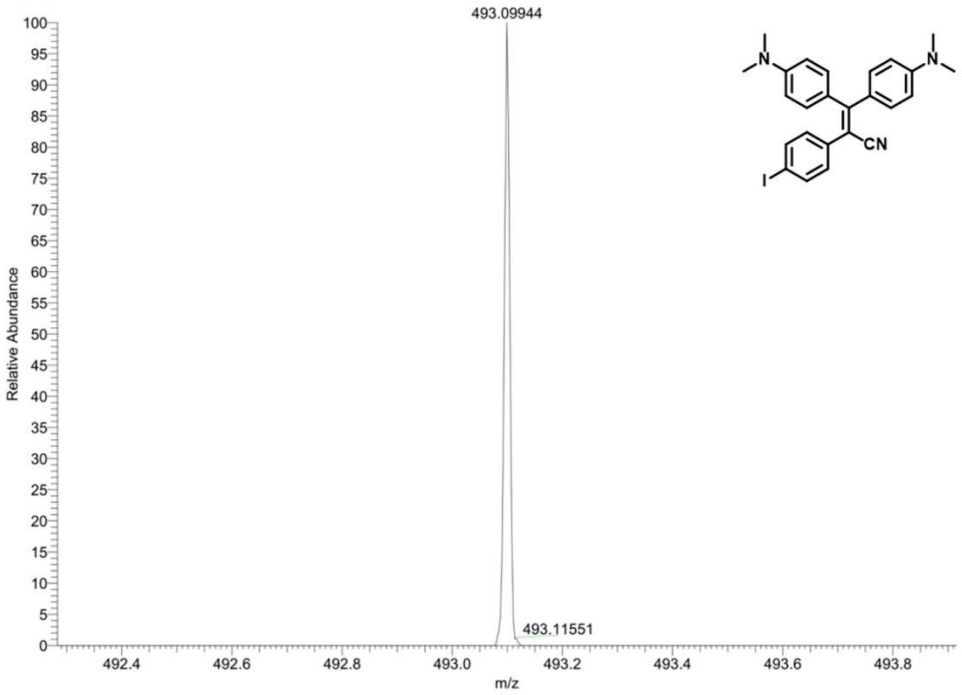

High-resolution mass spectrum of 3,3-bis(4-(dimethylamino)phenyl)-2-(4-iodophenyl)acrylonitrile(NTPAN-I)

6. References

(1) Wang, Y.; Yu, Y.; Liu, W.; Ren, L.; Ge, G. Exploration of highly efficient blue-violet light conversion agents for an agricultural film based on structure optimization of triphenylacrylonitrile. *J. Agric. Food Chem.* **2018**, *66*, 13295−13302.

(2) Frisch, M. J.; Trucks, G. W.; Schlegel, H. B.; Scuseria, G. E.; Robb, M. A.; Cheeseman, J. R.; Scalmani, G.; Barone, V.; Mennucci, B.; Petersson, G. A.; Nakatsuji, H.; Caricato, M.; Li, X.; Hratchian, H. P.; Izmaylov, A. F.; Bloino, J.; Zheng, G.; Sonnenberg, J. L.; Hada, M.; Ehara, M.; Toyota, K.; Fukuda, R.; Hasegawa, J.; Ishida, M.; Nakajiama, T.; Honda, Y.; Kitao, O.; Nakai, H.; Vreven, T.; Montgomery, J. A., Jr.; Peralta, J. E.; Ogliaro, F.; Bearpark, M.; Heyd, J. J.; Borthers, E.; Kudin, K. N.; Staroverov, V. N.; Kobayashi, R.; Normand, J.; Rahavachari, K.; Rendell, A.; Burant, J. C.; Iyengar, S. S.; Tomasi, J.; Cossi, M.; Rega, N.; Millam, J. M.; Klene, M.; Knox, J. E.; Cross, J. B.; Bakken, V.; Adamo, C.; Jaramillo, Gomperts, R.; Stratmann, R. E.; Yazyev, O.; Austin, A. J.; Cammi, R.; Pomelli, C.; Ochterski, J. W.; Martin, R. L.; Morokuma, K.; Zakrzewski, V. G.; Voth, G. A.; Salvador, P.; Dannenberg, J. J.; Dapprich, S.; Daniels, A. D.; Farkas, O.; Foresman, J. B.; Ortiz, J. V.; Cioslowski, J.; Fox, D. J. Gaussian, Inc. Wallingford CT, **2009**.

(3) Becke, A. D. Density-functional thermochemistry. III. The role of exact exchange. *J. Chem. Phys.* **1993**, *98*, 5648−5652.

(4) Adamo, C.; Jacquemin, D. The calculations of excited-state properties with time-dependent density functional theory. *Chem. Soc. Rev.* **2013**, *42*, 845−856.

(5) (a) C. Lefebvre, G. Rubez, H. Khartabil, J.-C. Boisson, J. Contreras-Garca, E. Hnon, *Phys. Chem. Chem. Phys.* **2017**, 19, 17928-17936; (b) T. Lu, F. *Chen, J. Comput. Chem*. **2012**, 33, 580-592.

(6) M. J. Turner, J. J. McKinnon, S. K. Wolff, D. J. Grimwood, P. R. Spackman, D. Jayatilaka and M. A. Spackman, *CrystalExplorer17* (**2017**). University of Western Australia.